Impacts of Particulate Ingestion on External and Internal Flow Paths

Karen A. Thole

Department of Mechanical and Nuclear Engineering

Experimental and Computational Convection Lab

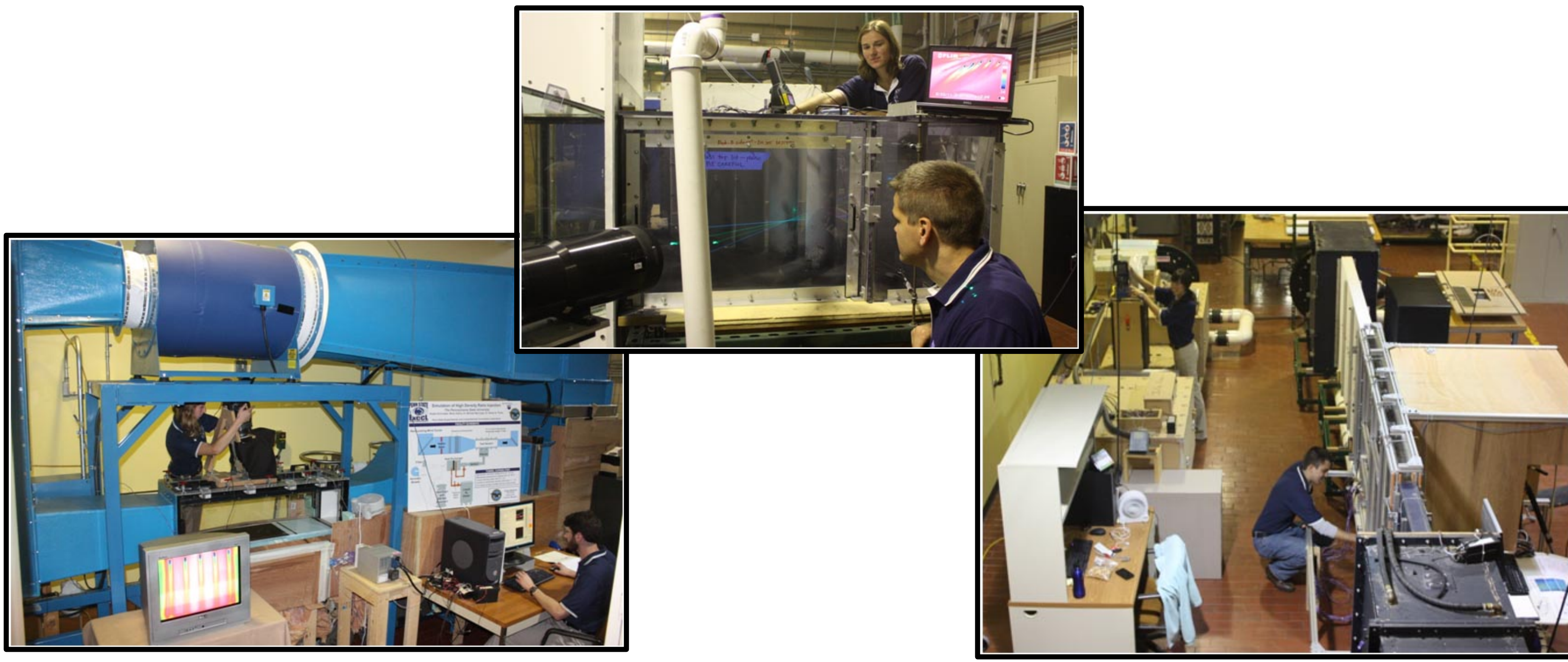

The presentation will cover several items related to aero-heat transfer experiments done at Penn State

Introduction to facilities at Penn State

Particle deposition on external surfaces

Particle deposition on internal surfaces

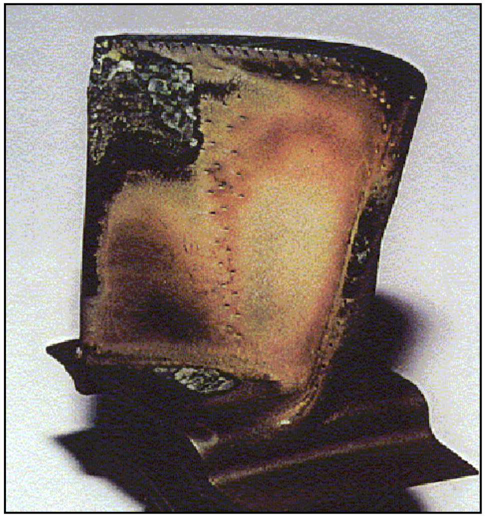

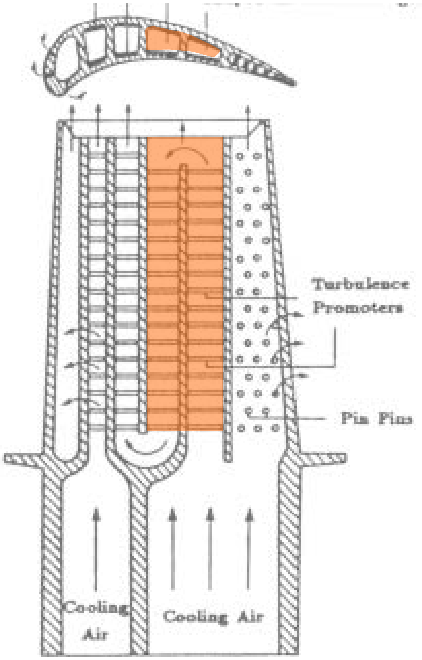

Han et al.

Several flow facilities are available in the PSUExCCL

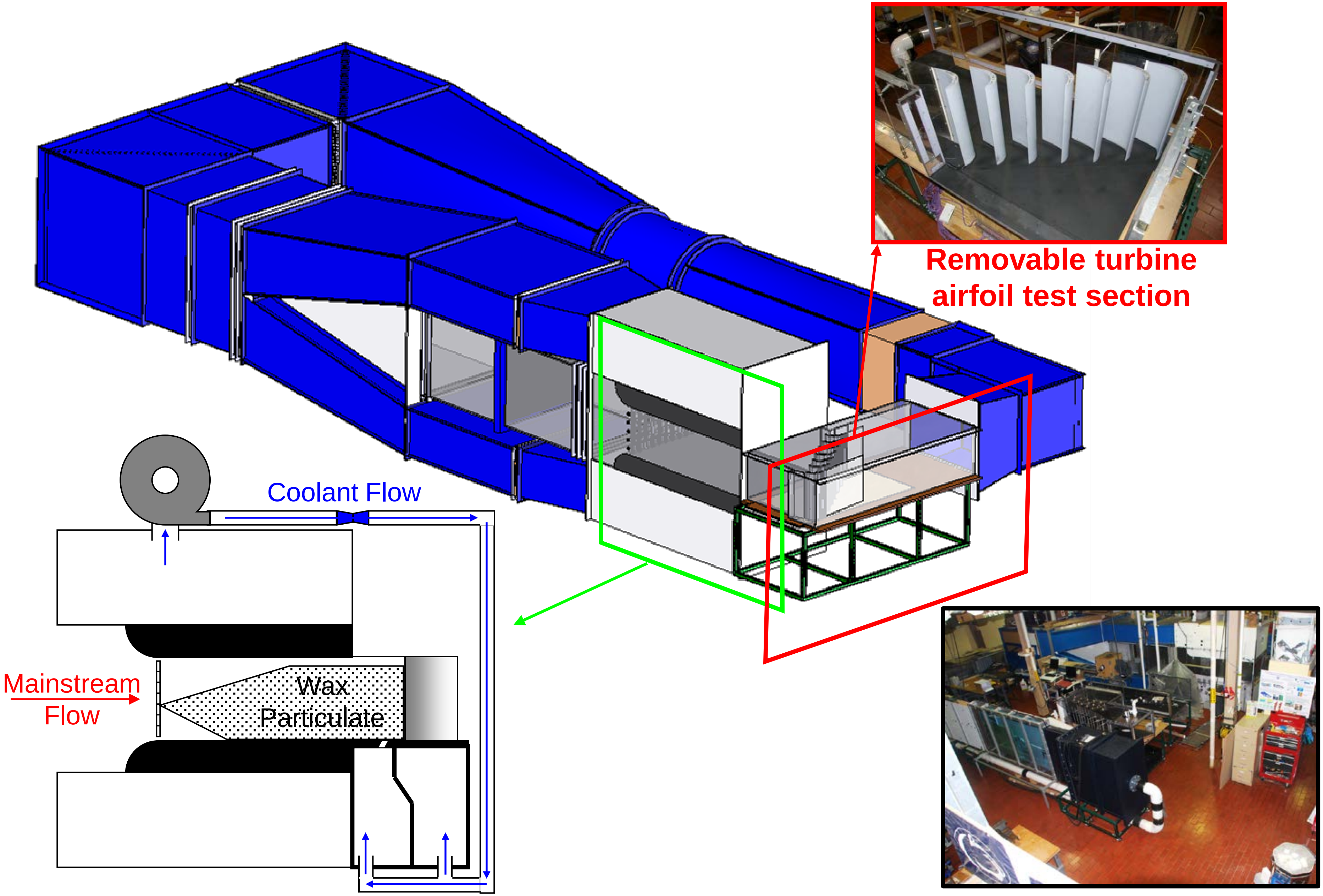

Several flow facilities are available in the PSUExCCL

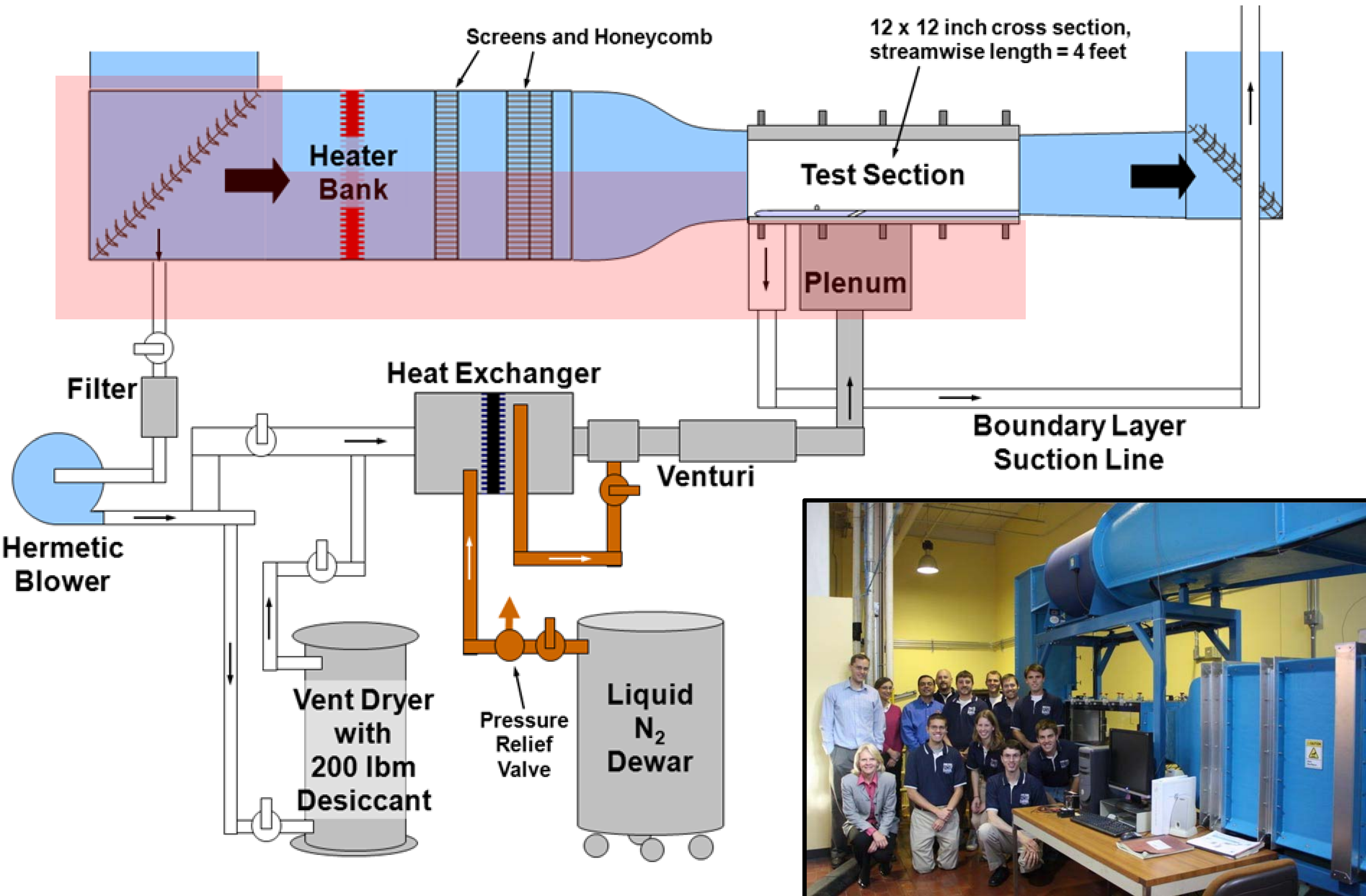

Several flow facilities are available in the PSUExCCL

Flowfield Facility

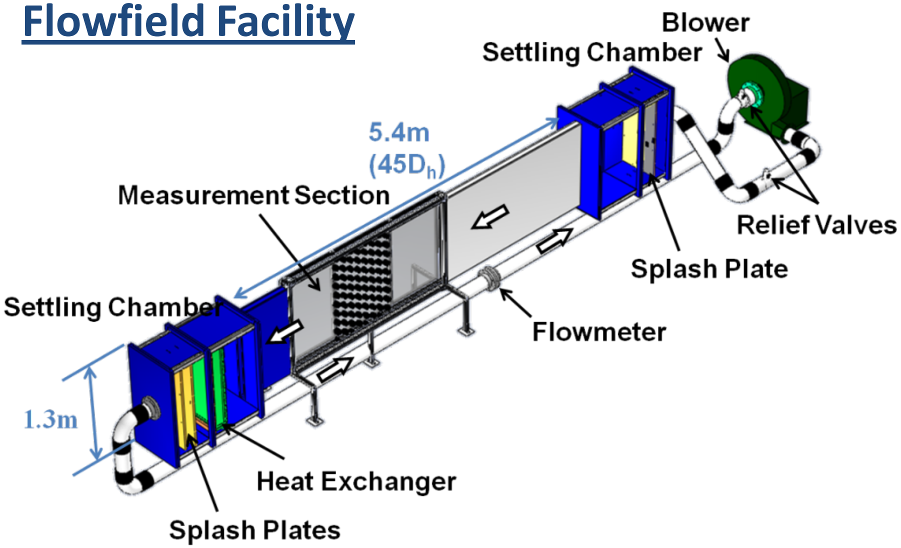

Features:

64x

Glass/polycarbonate test section

Optical access in visible light spectrum

PIV measurements

Heat Transfer Facility

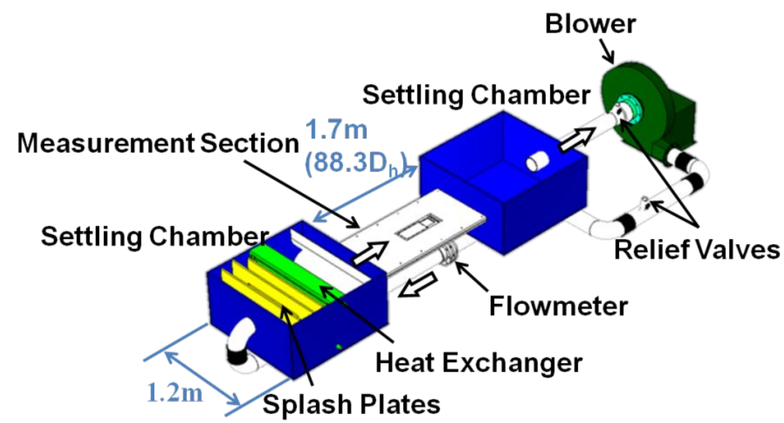

Features:

10x

MDF test section

Cutout for Zinc-Selenide window

Optical access in IR spectrum

IR thermography measurements

A test facility was developed to investigate rust injection at rotating conditions

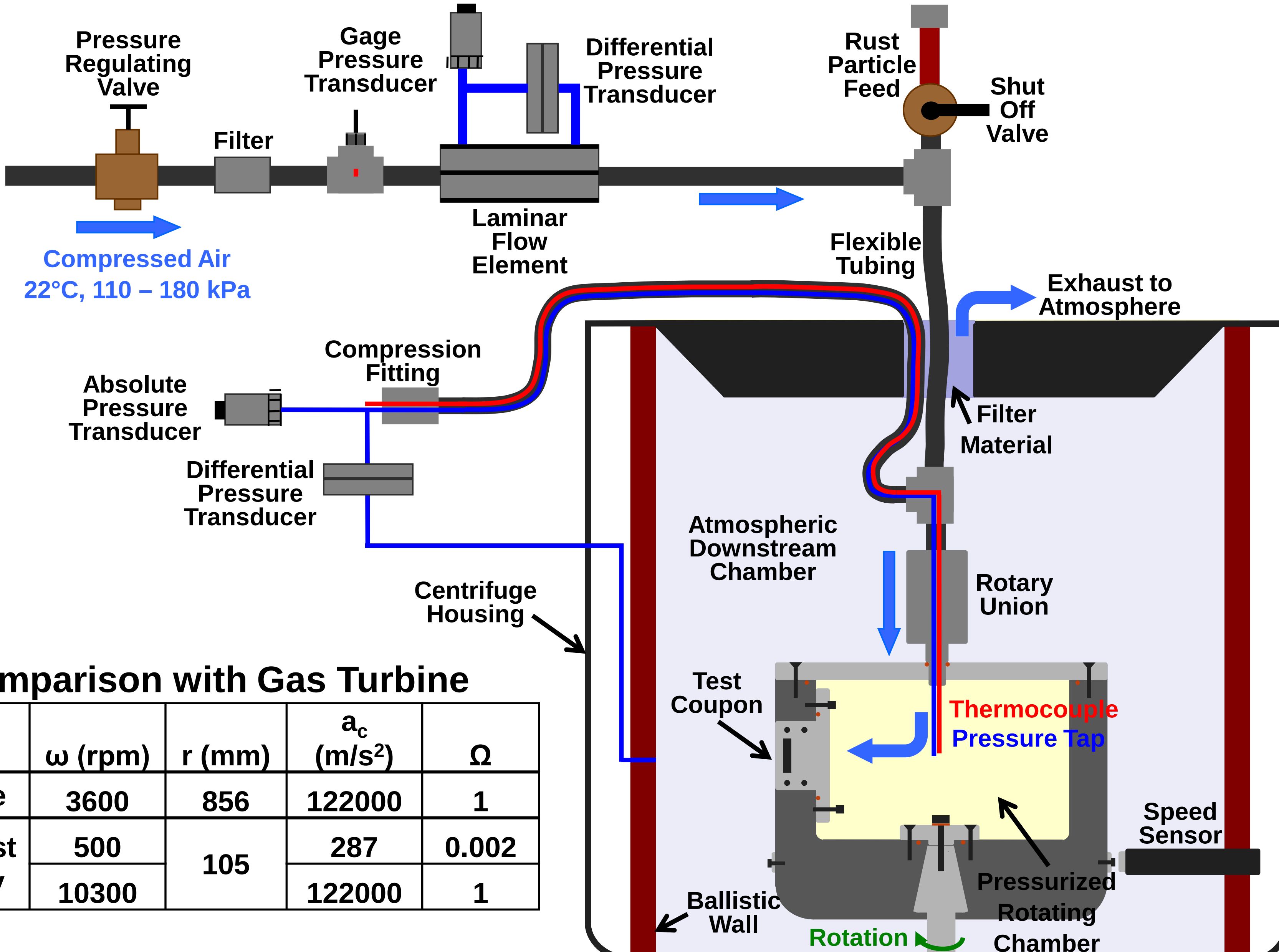

Comparison with Gas Turbine

	ω (rpm)	r (mm)	a_c (m/s^2)	Ω
Turbine	3600	856	122000	1
PSU Test Facility	500	105	287	0.002
	10300		122000	1

Flowfield measurements are made using time-resolved PIV

PIV orientation in facility

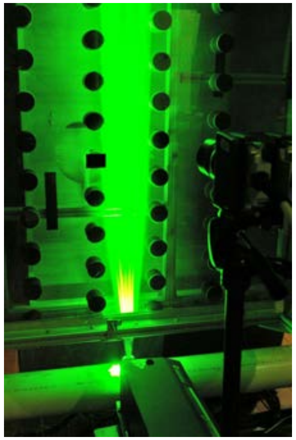

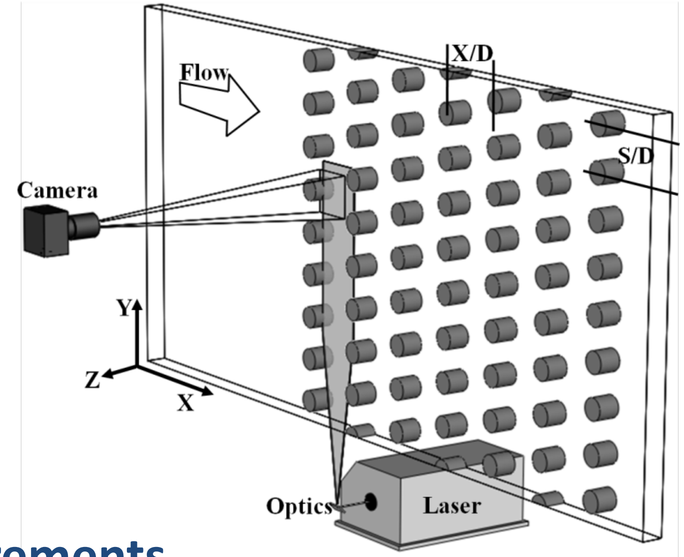

Wake measurements

Constant Z/H = 0 (channel symmetry plane)

Basics of PIV operation

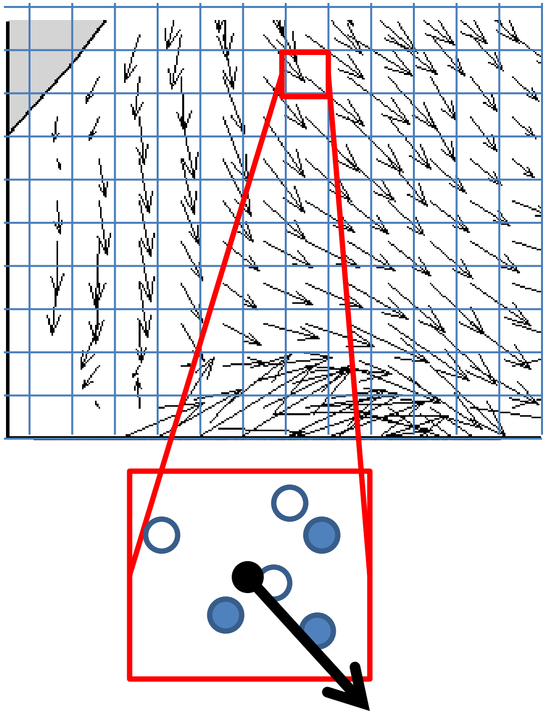

Time-resolved:

1000 Hz

500 Hz Nyquist

30x shedding frequency at Re = 2.0e4

Spatially-resolved:

1024x1024px

125mm x 125mm viewing area

7.6 pixels/mm

y^+ = 5 (between vectors)

Statistical convergence:

3000 samples

(1000 for convergence)

Flow crosses domain minimum 60 times

Heat transfer measurements are made with IR thermography

IR Camera orientation in facility

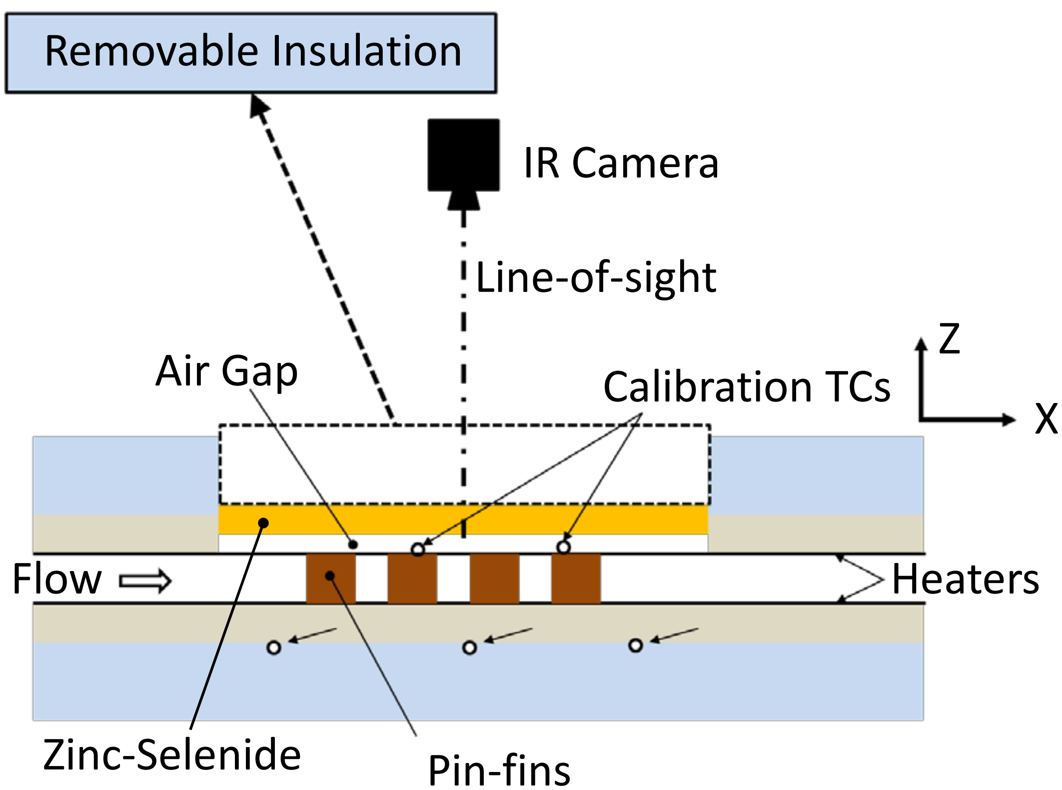

Constant heat flux method

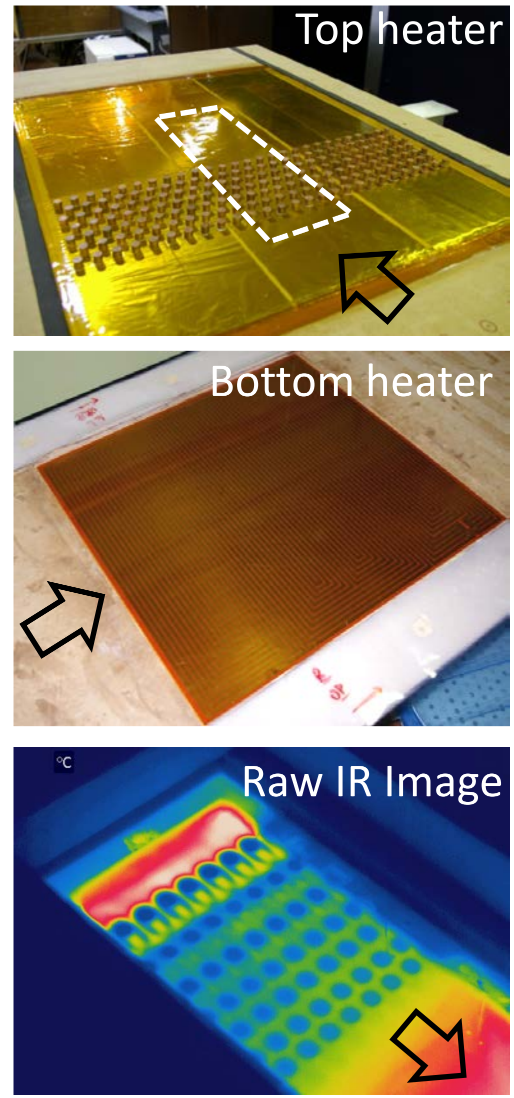

We need to gain a better understanding of the effects of particle deposition

Aircraft Applications

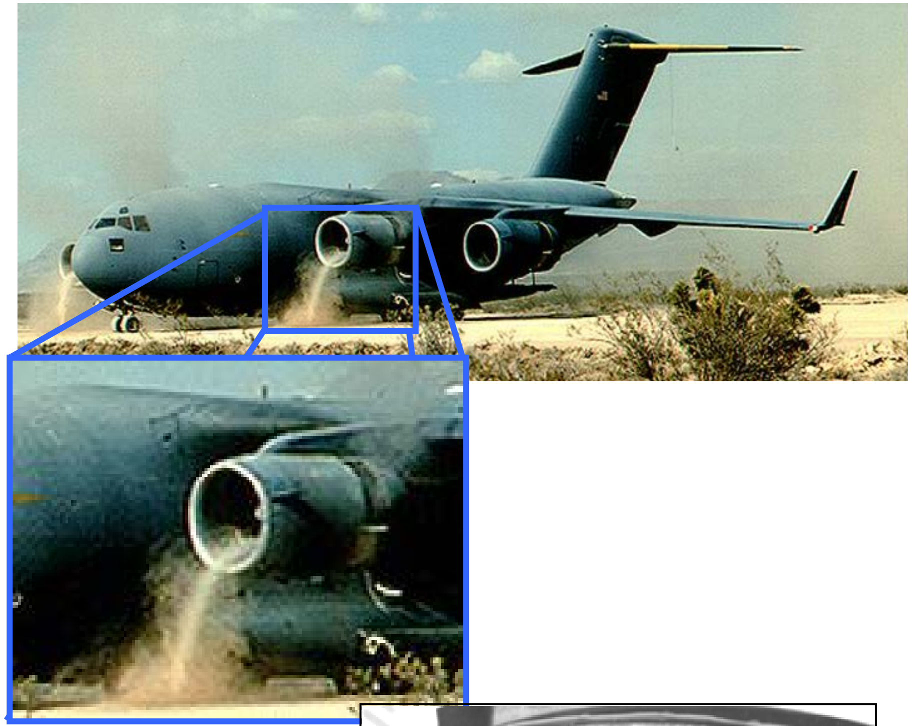

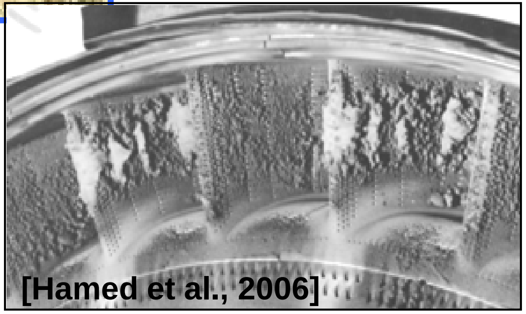

[Hamed et al., 2006]

Land Based Applications

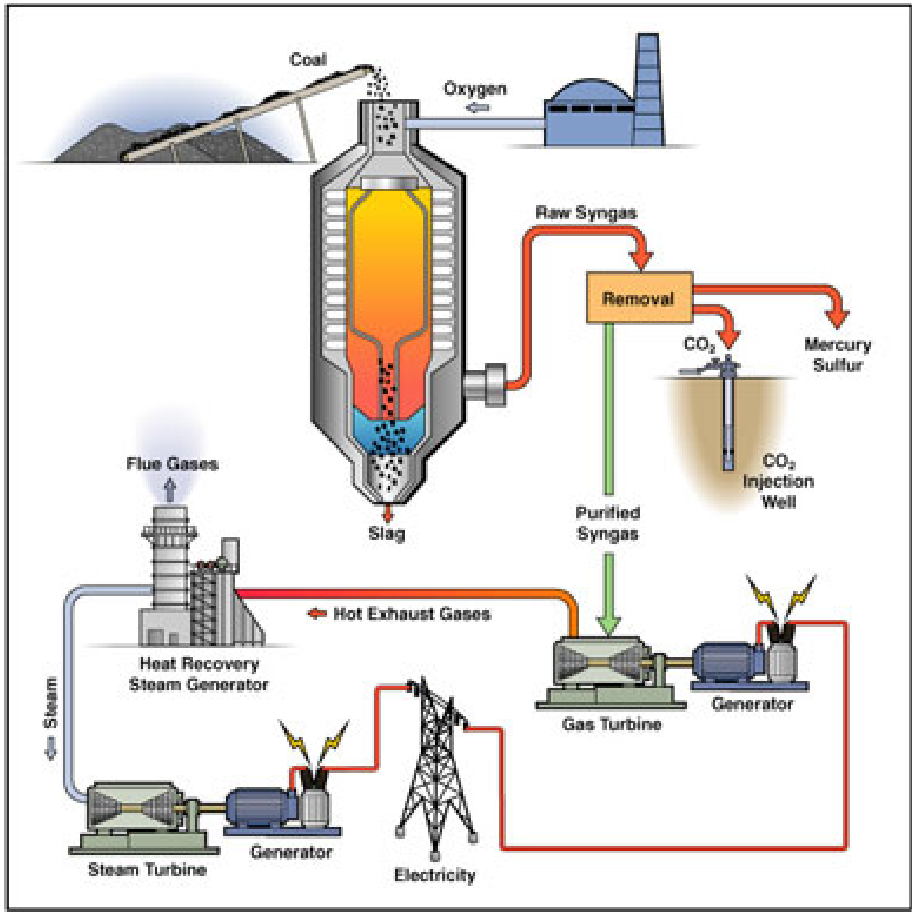

Dynamically simulate particle deposition on <u>external</u> and <u>internal</u> surfaces to determine effects on cooling

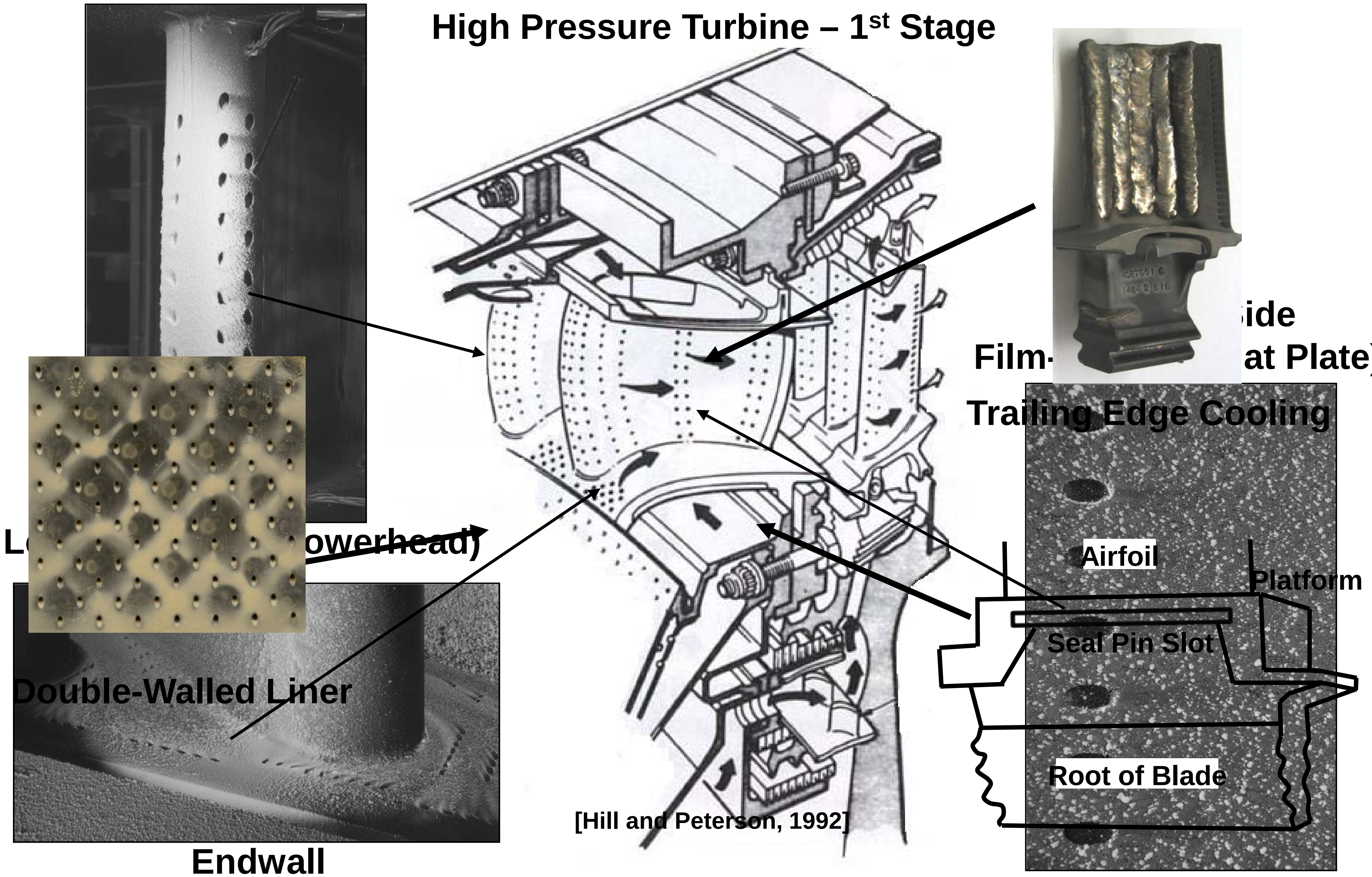

This presentation covers aspects related to dirt, dust, and rust on external and internal flow paths

External Flow Path

- Scaling issues
- Simulation methods
- Results for three regions

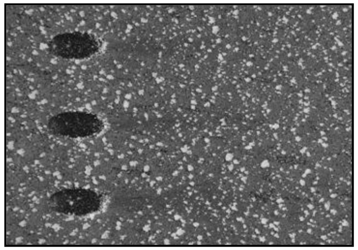

Film-Cooling

Showerhead

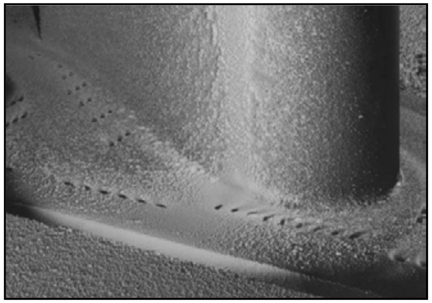

Endwall

Internal Flow Path

- Scaling issues
- Simulation methods
- Results for two regions

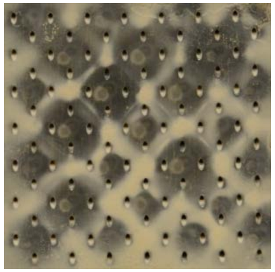

Double-Walled Liner

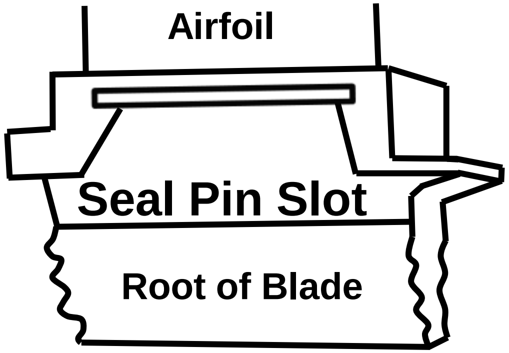

Particle motion and particle phase must be properly scaled from engine to laboratory conditions

Particle Motion

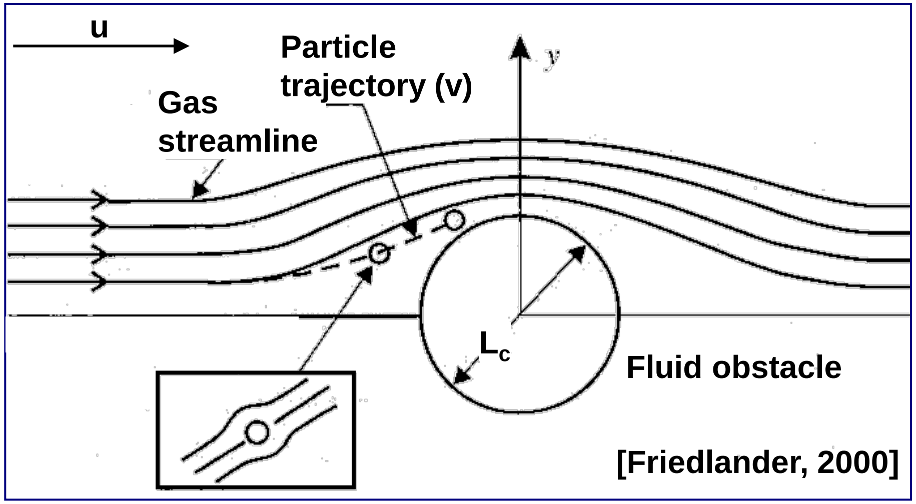

$$\tau_p = \frac{\rho_p d_p^2}{18\mu}$$

$$\tau_f = \frac{L_c}{U}$$

$$\boxed{Stk = \frac{\tau_p}{\tau_f}}$$

Stk<<1 particle follows streamlines

Stk>>1 particle trajectory dominated by particle inertia

Particle Phase

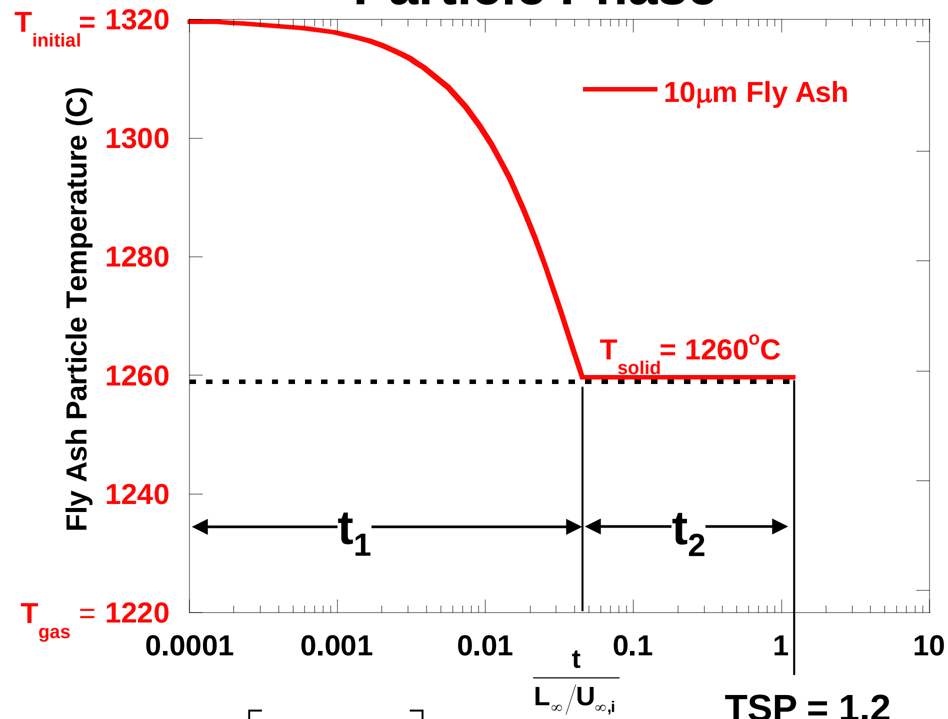

TSP = 1.2

$$t_1 = -\frac{\rho_p C_p V_p}{hA_p} \ln\left[\frac{T_{p,s} - T_\infty}{T_{p,i} - T_\infty}\right]$$

$$t_2 = \frac{\Delta H_{fus}}{hA_p\left(T_{p,s} - T_\infty\right)}$$

$$\boxed{TSP = \frac{t_1 + t_2}{L_\infty / U_{\infty,i}}}$$

TSP < 1 Solid (S)

TSP > 1 Molten (M)

L_∞ = distance from combustor to turbine surface

$U_{\infty,i}$ = inlet mainstream velocity

Dynamically simulate particle deposition on <u>external</u> surfaces to determine effects on cooling

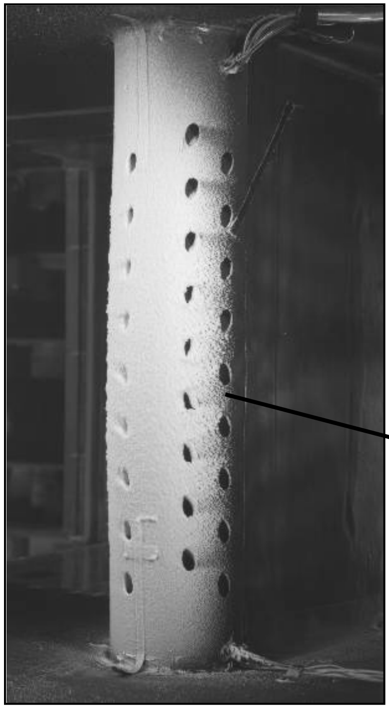

Leading Edge (Showerhead)

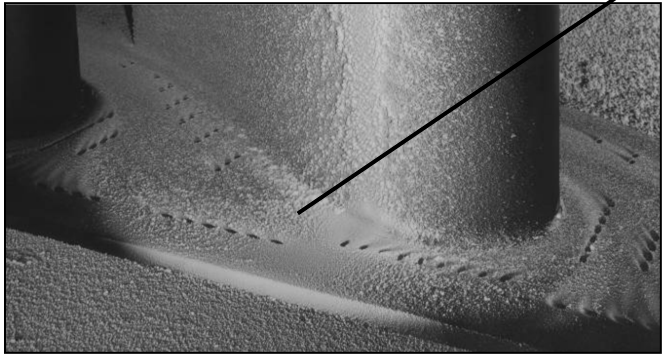

Endwall

High Pressure Turbine – 1st Stage

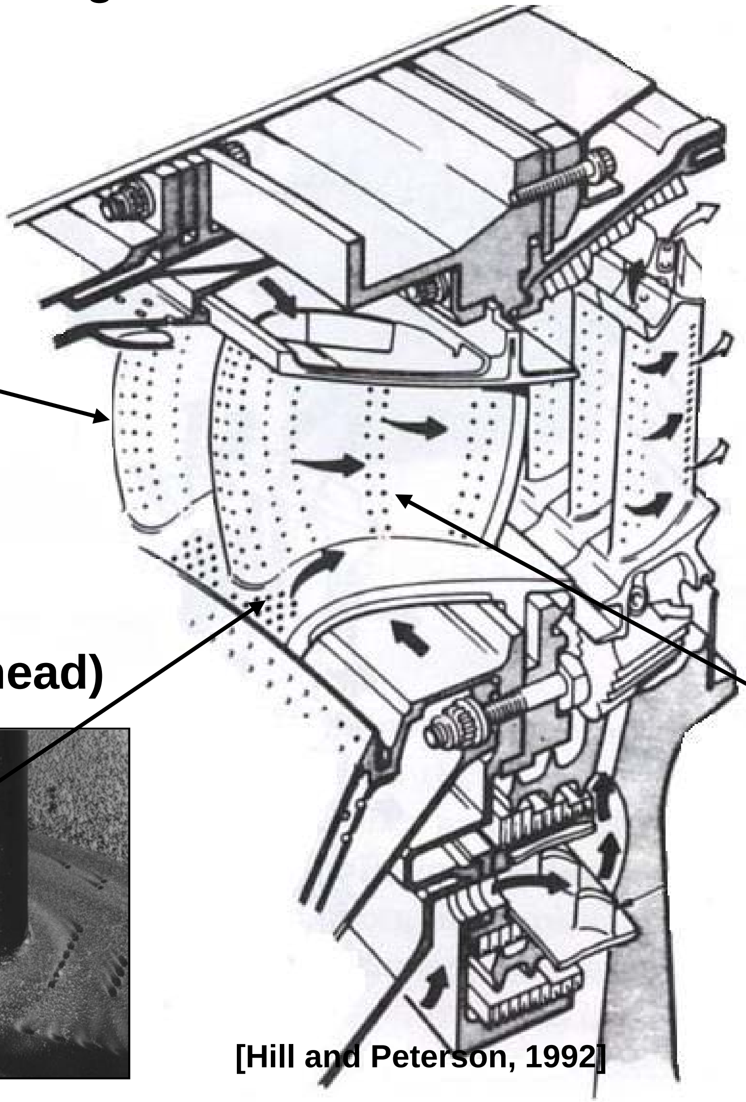

[Hill and Peterson, 1992]

Pressure Side
Film-Cooling (Flat Plate)

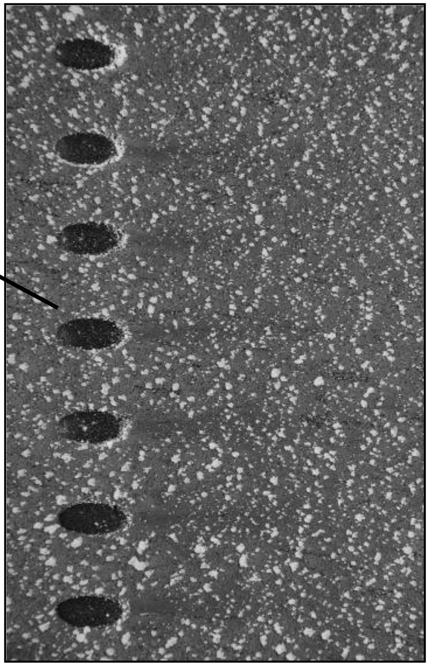

Wax was injected in different stages to observe deposition and effectiveness development

I = 0.23
M = 0.50

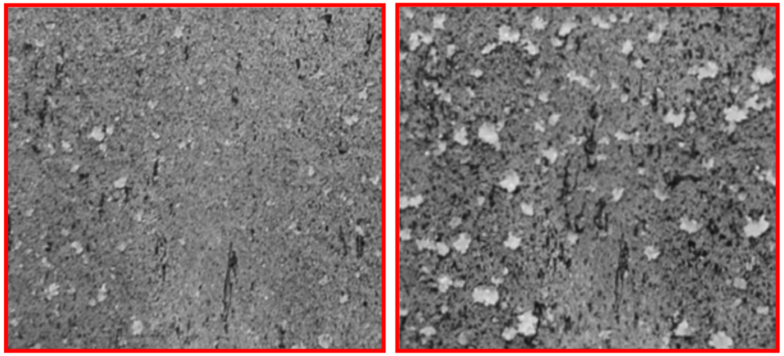

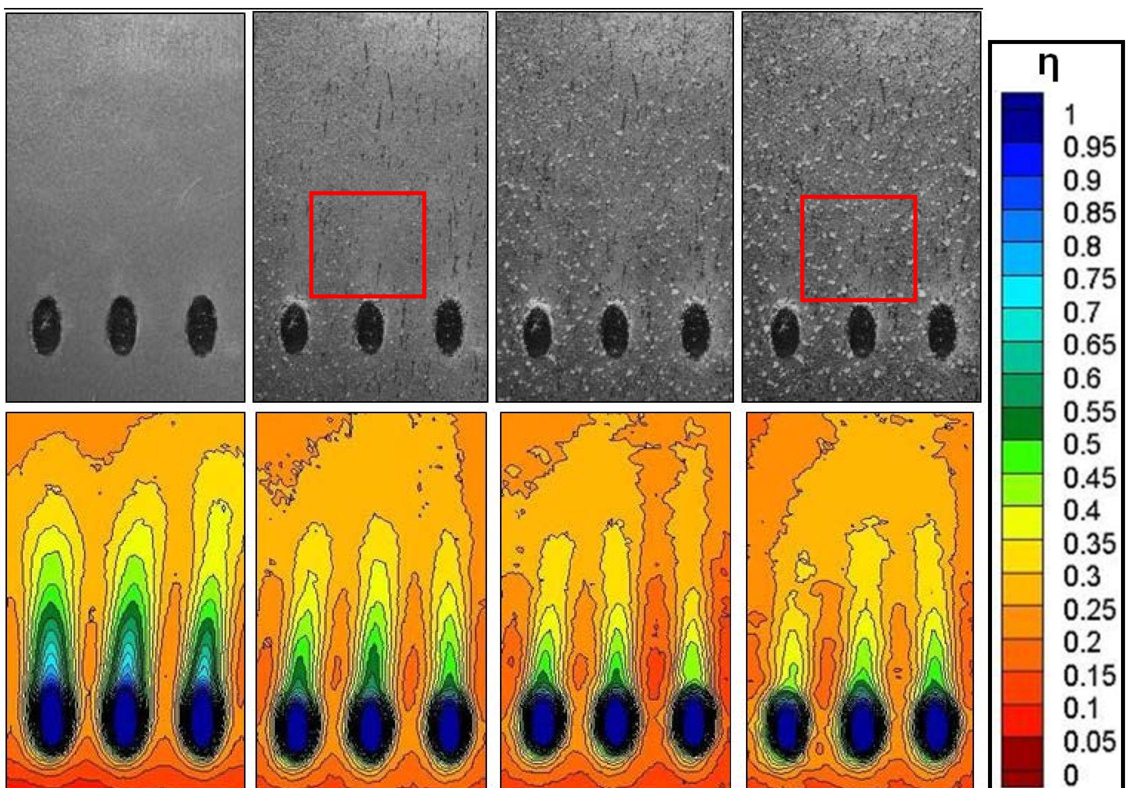

Before Deposition | **After 1200g** | **After 2400g** | **After 3200g**

Initially, only large molten particles deposit

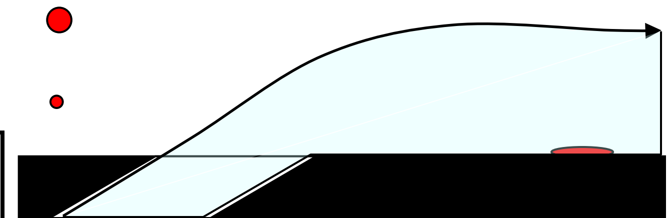

Eventually, small solid particles stick to existing deposits

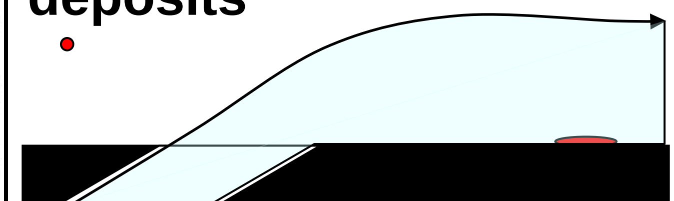

Effectiveness reduction approached an equilibrium state as deposition area coverage increased

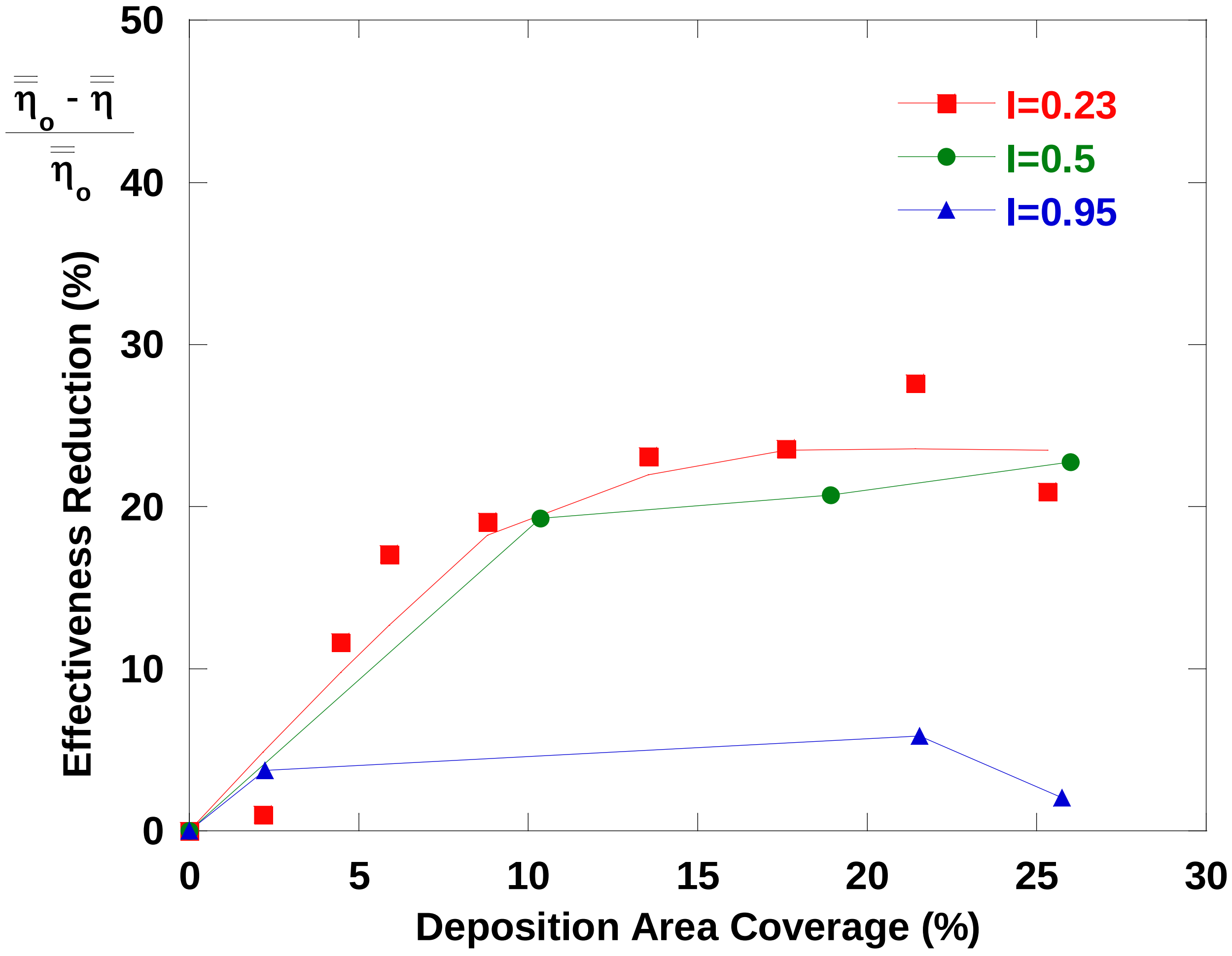

Deposition within leading edge cooling holes decreased with an increase in blowing ratio

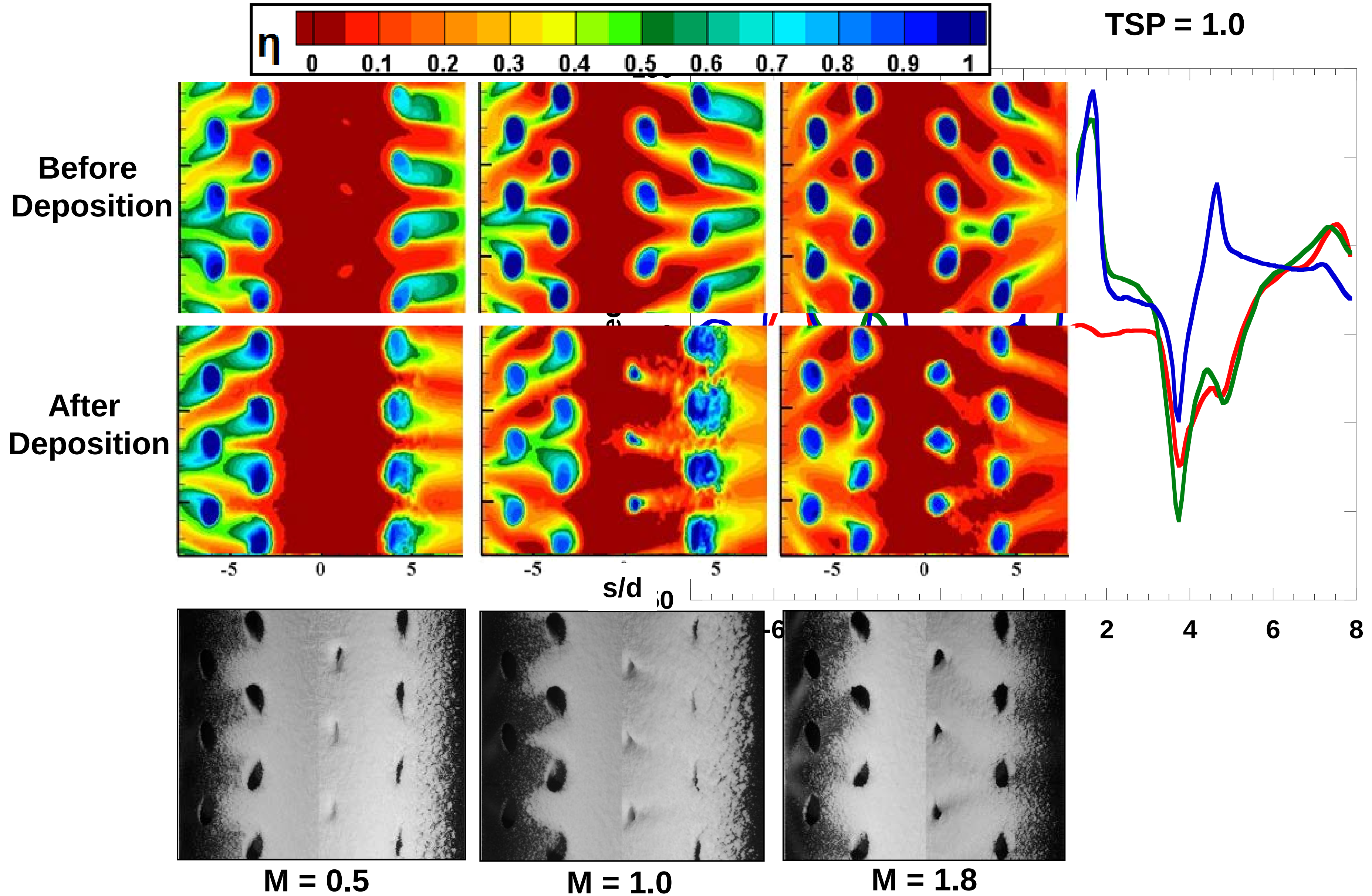

All three trench depths reduced the negative impact of deposition on endwall cooling effectiveness

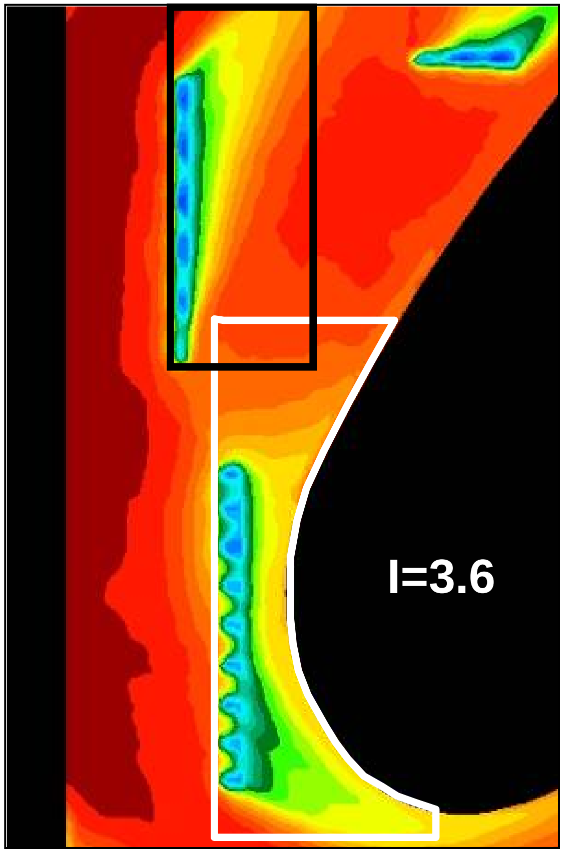

0.8d Trench

$$\bar{\bar{\eta}}_{total} = \frac{A_{passage}\bar{\bar{\eta}}_{passage} + A_{LE}\bar{\bar{\eta}}_{LE}}{A_{passage} + A_{LE}}$$

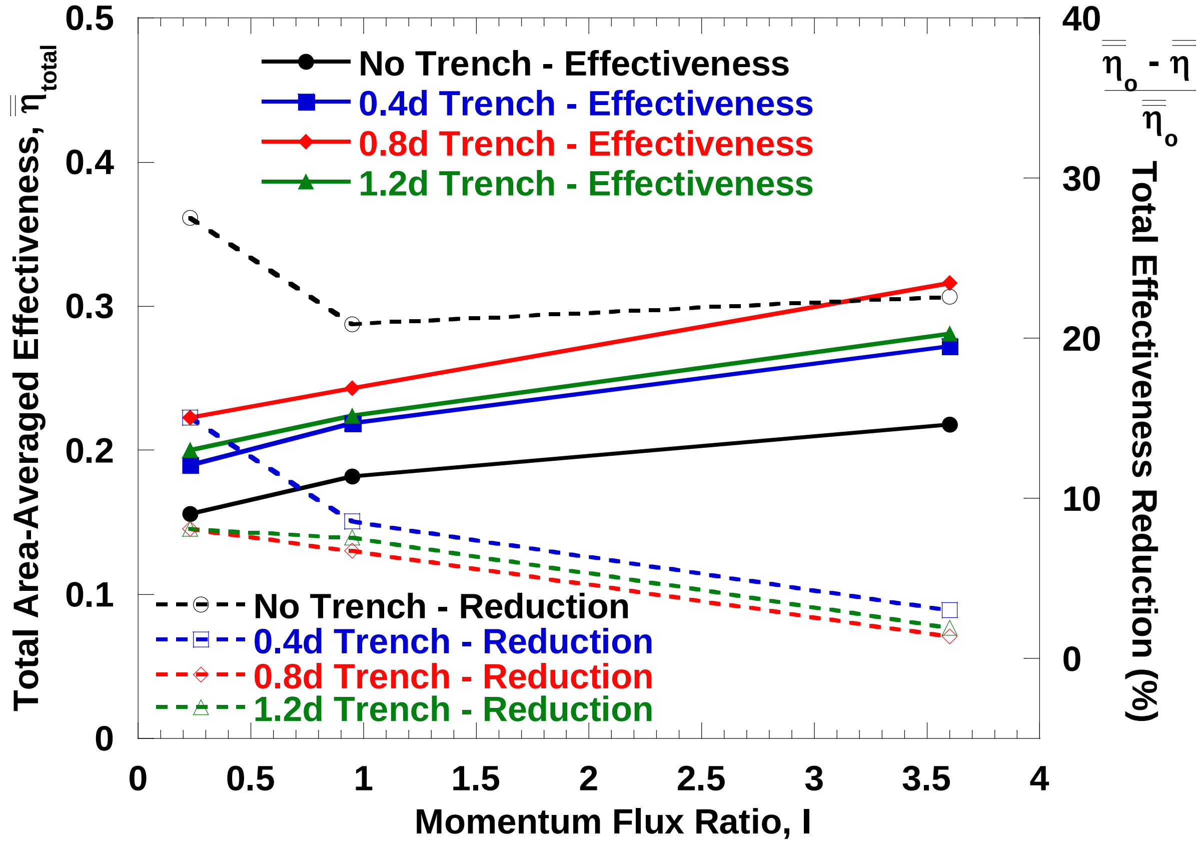

Contouring can alter cooling patterns and lead to deposition regions

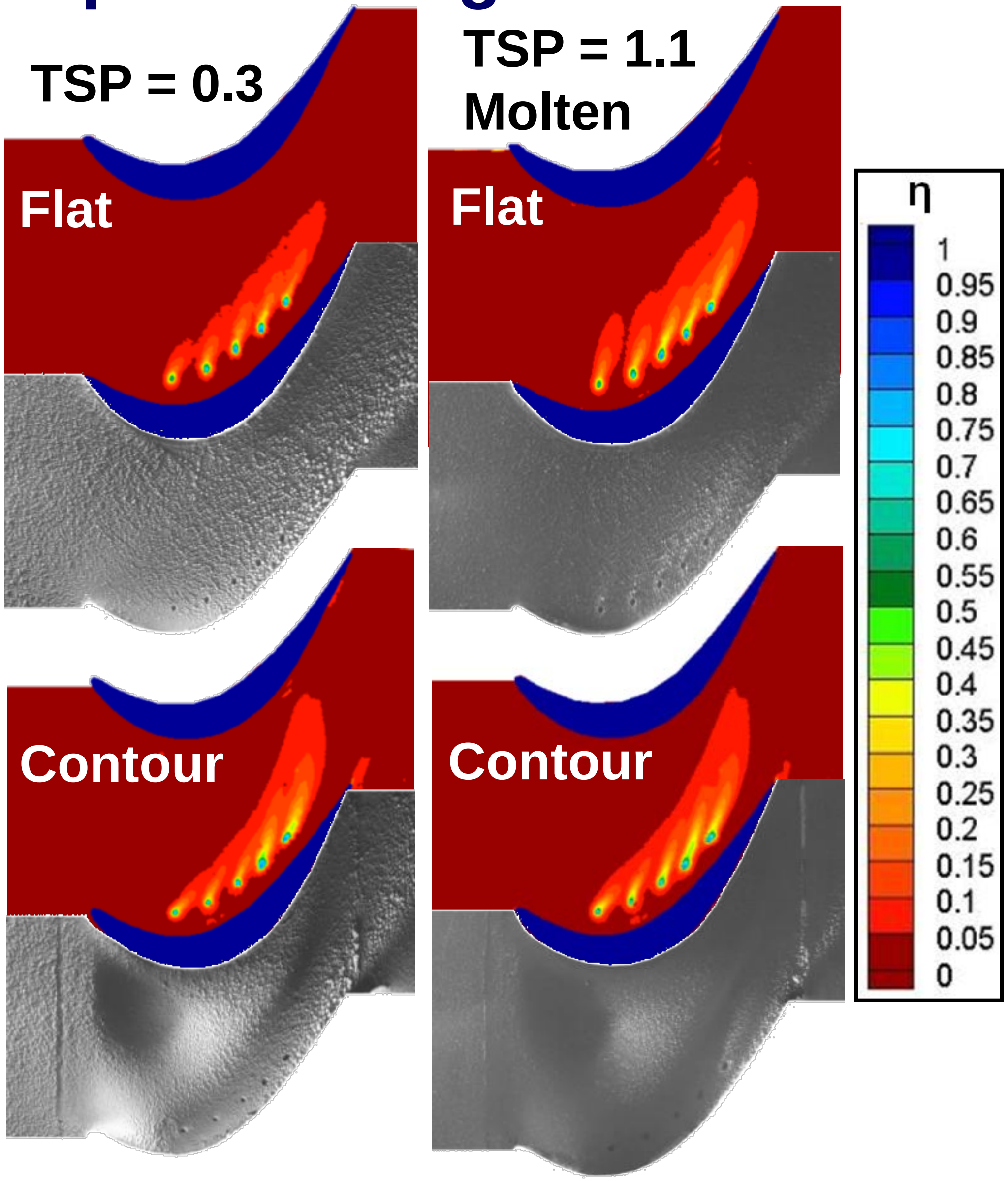

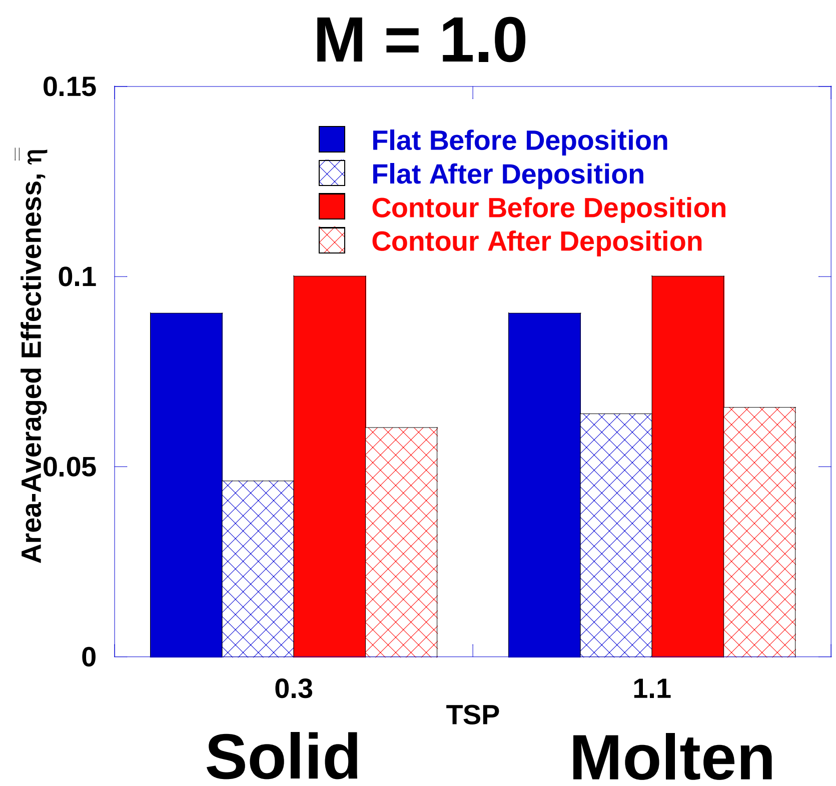

Experimental deposition patterns were similar to computationally predicted accretion rates

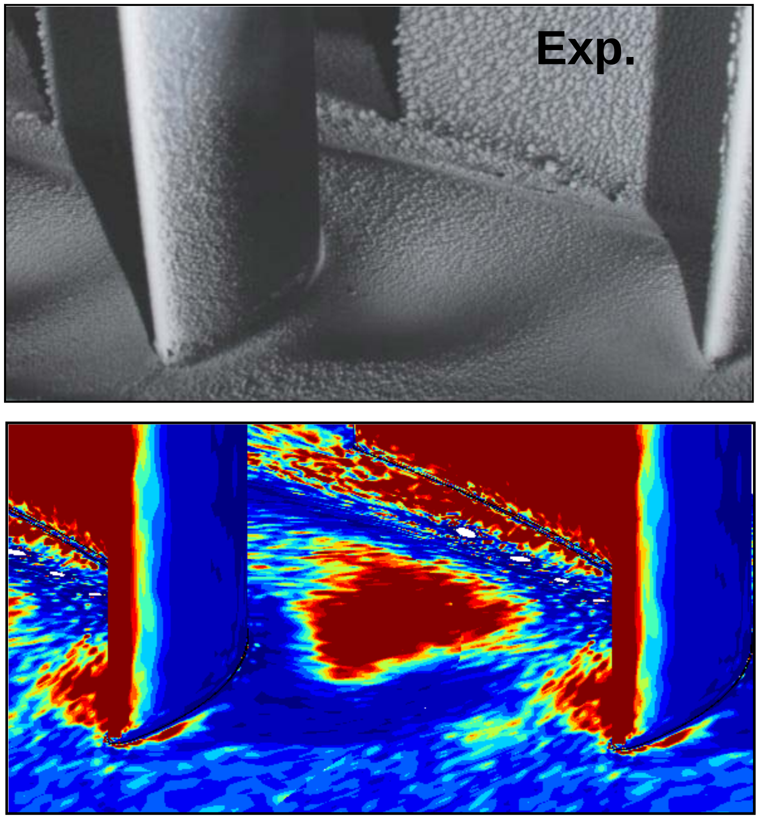

M = 1.0

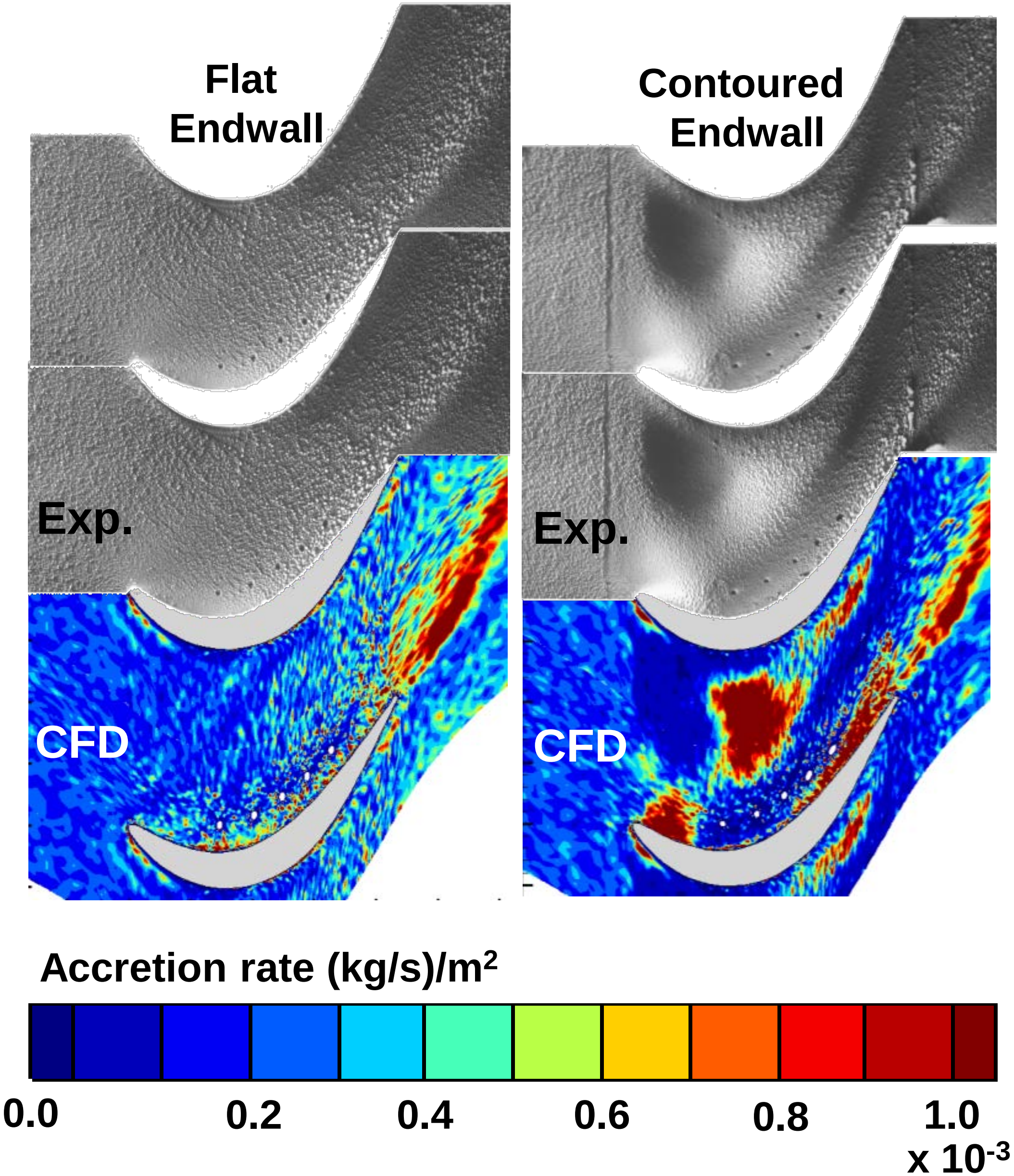

Effects of deposition on cooling varied with location

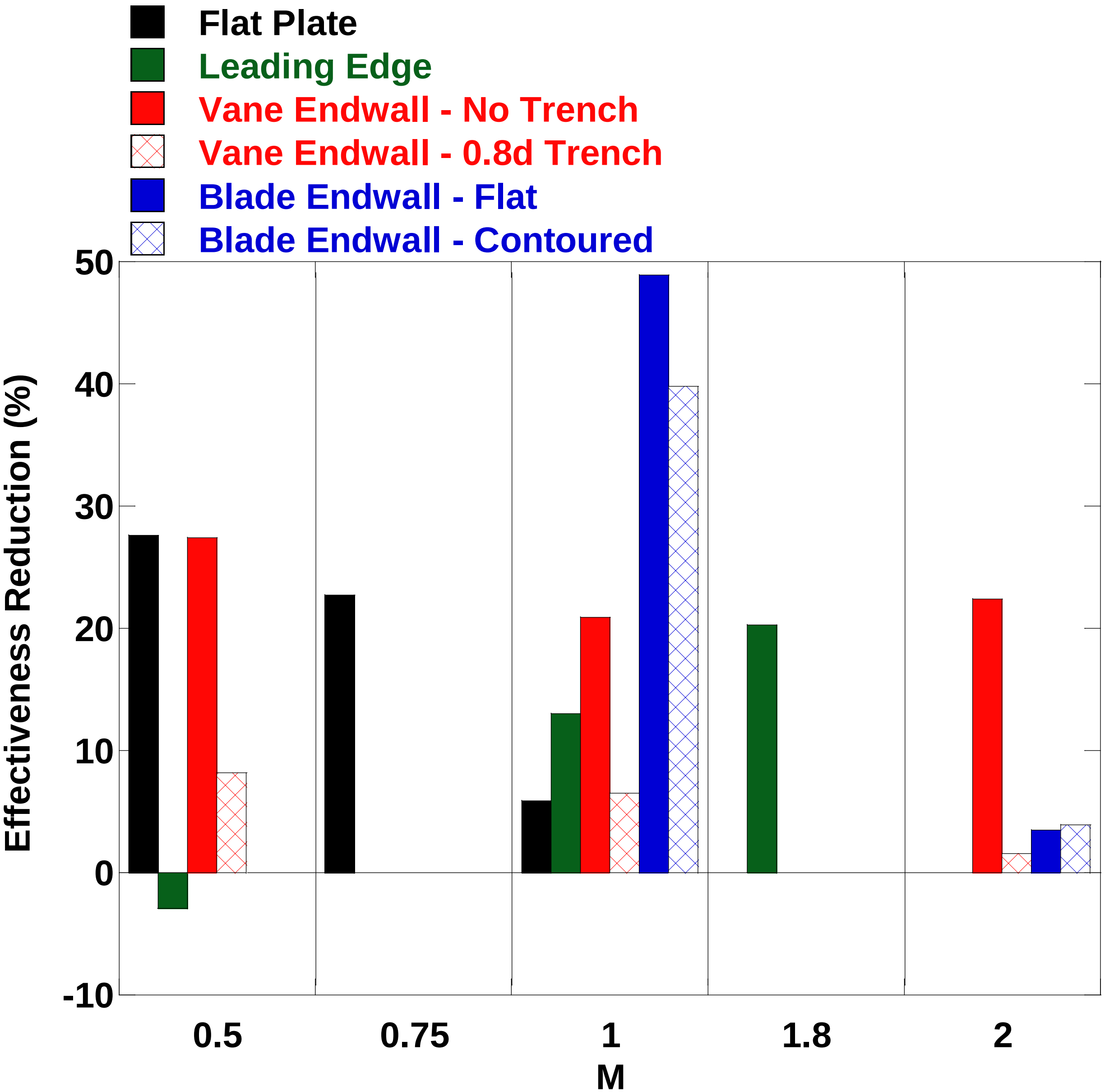

Dynamically simulate particle deposition on <u>internal</u> surfaces to determine blockage effects and heat transfer implications

High Pressure Turbine – 1st Stage

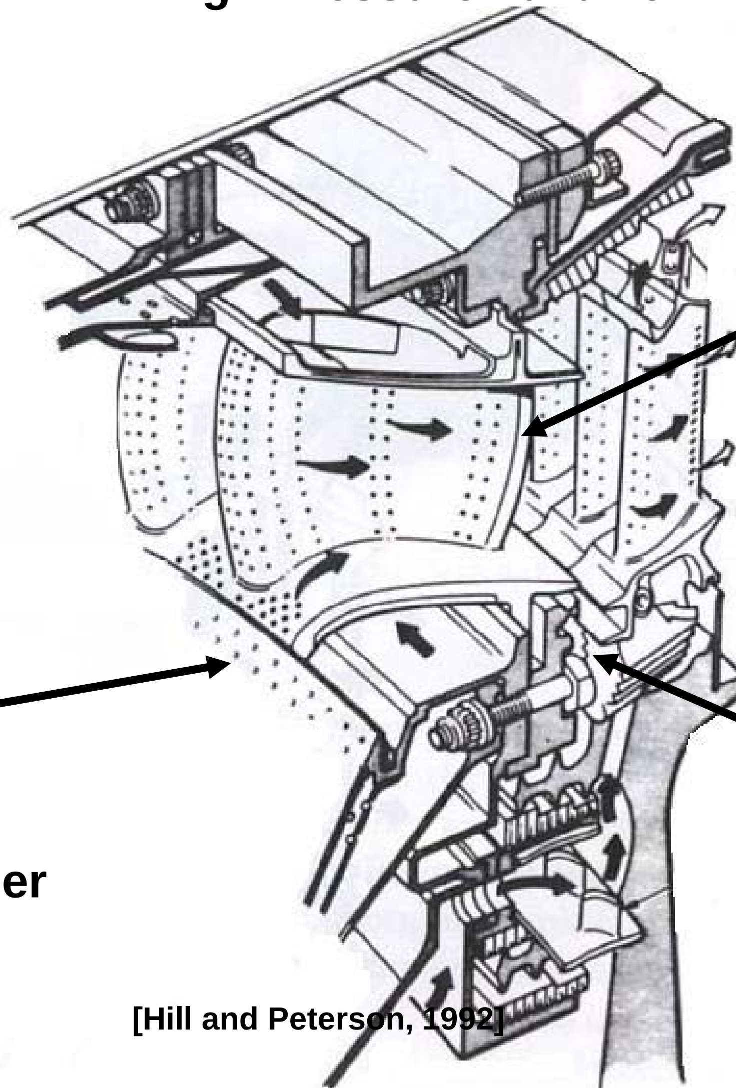

[Hill and Peterson, 1992]

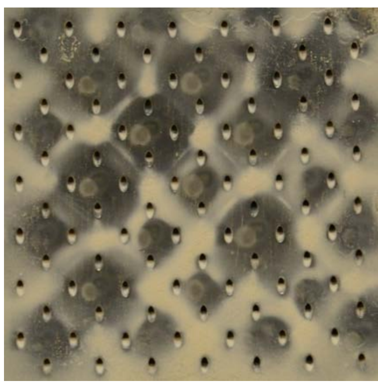

Double-Walled Liner

Trailing Edge Cooling

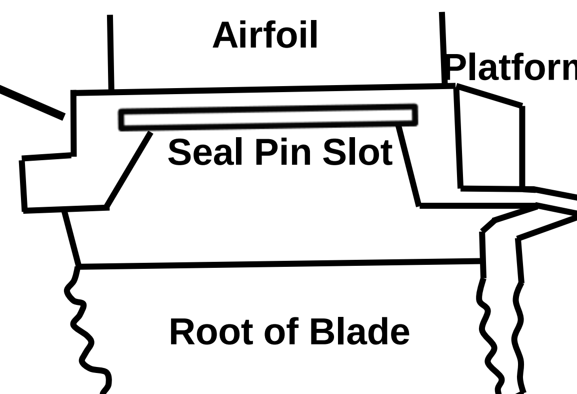

Injection sand amounts were determined based on field hardware

0.014 in Film Holes, Forward Cavity, $0<D_S<0.15$ in Sand

$$\%RFF = \frac{FF_0 - FF}{FF_0}$$

$$FF = \frac{\dot{m}\sqrt{T_{0C}}}{P_\infty}$$

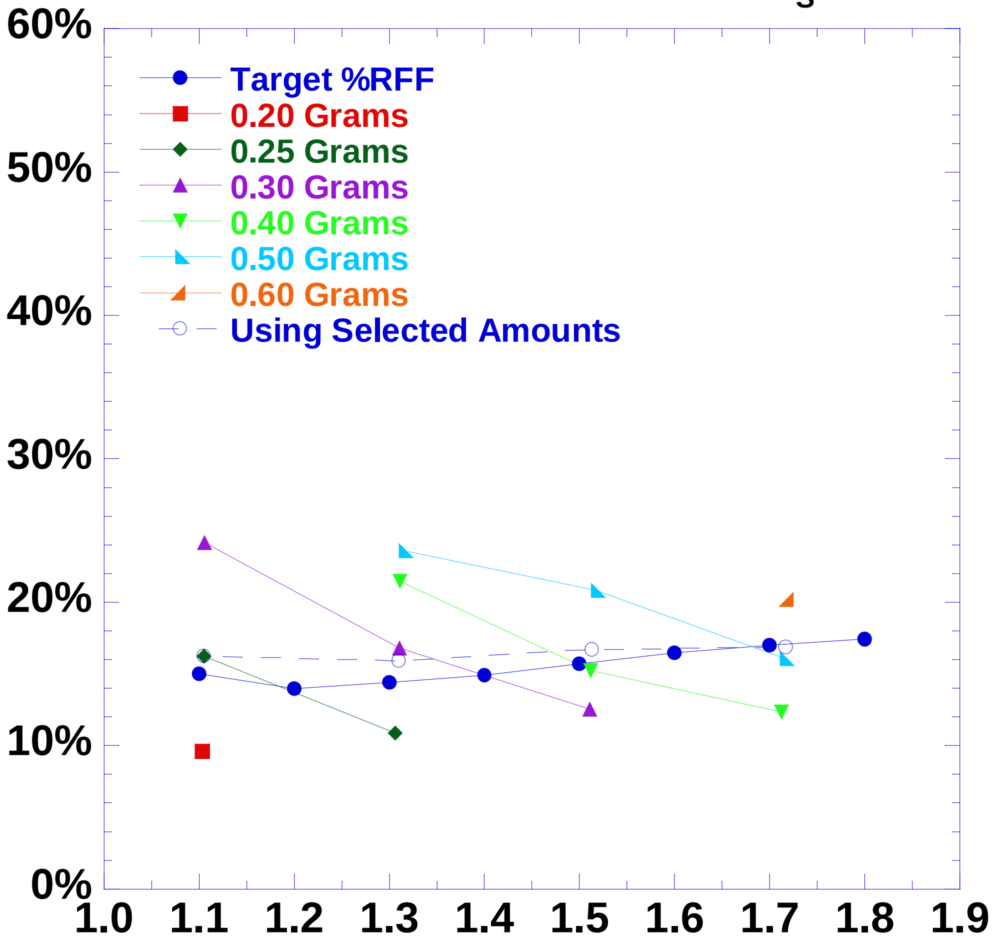

$$PR = \frac{P_{0C}}{P_\infty}$$

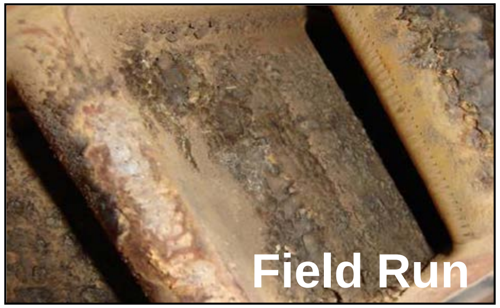

Sand diameter causes the melting point to be lower than is reported for this chemical substance

Room Temperature

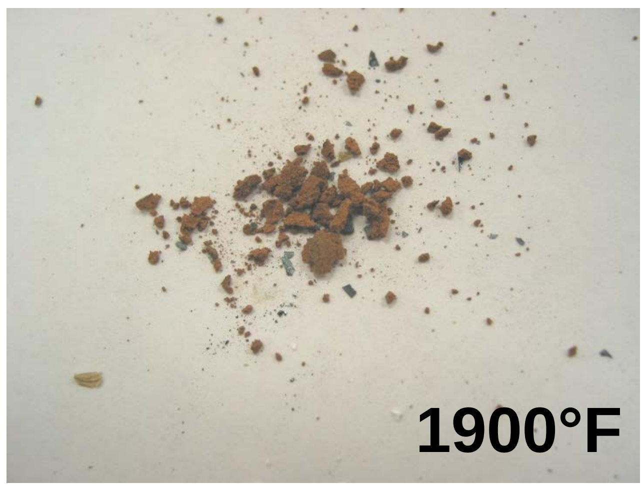

Reported Melting Temperature

2930°F [Incropera & DeWitt]

3130°F [Handbook of Chem. & Phys.1981]

The impingement jets and film-cooling jets were tested both staggered and aligned

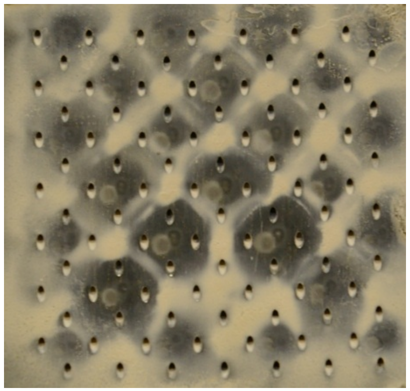

Staggered

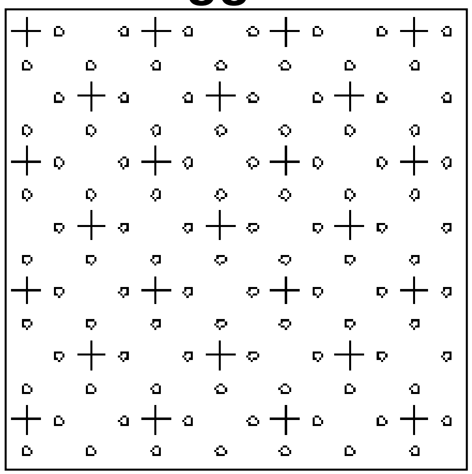

Aligned

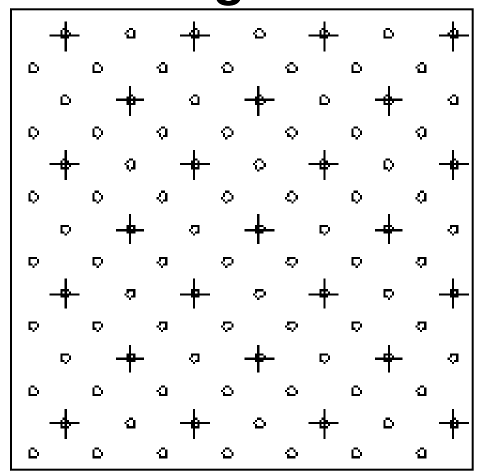

+ = impingement holes
o = film-cooling holes

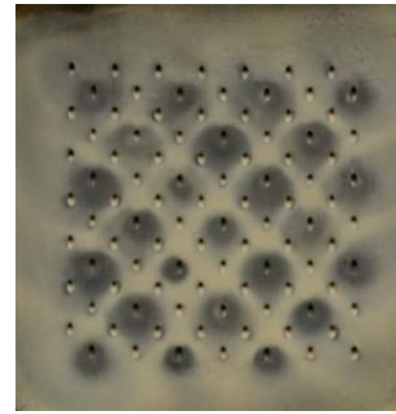

The S/D = 3.1 had less blockage due to decreased crossflow and decreased jet spreading

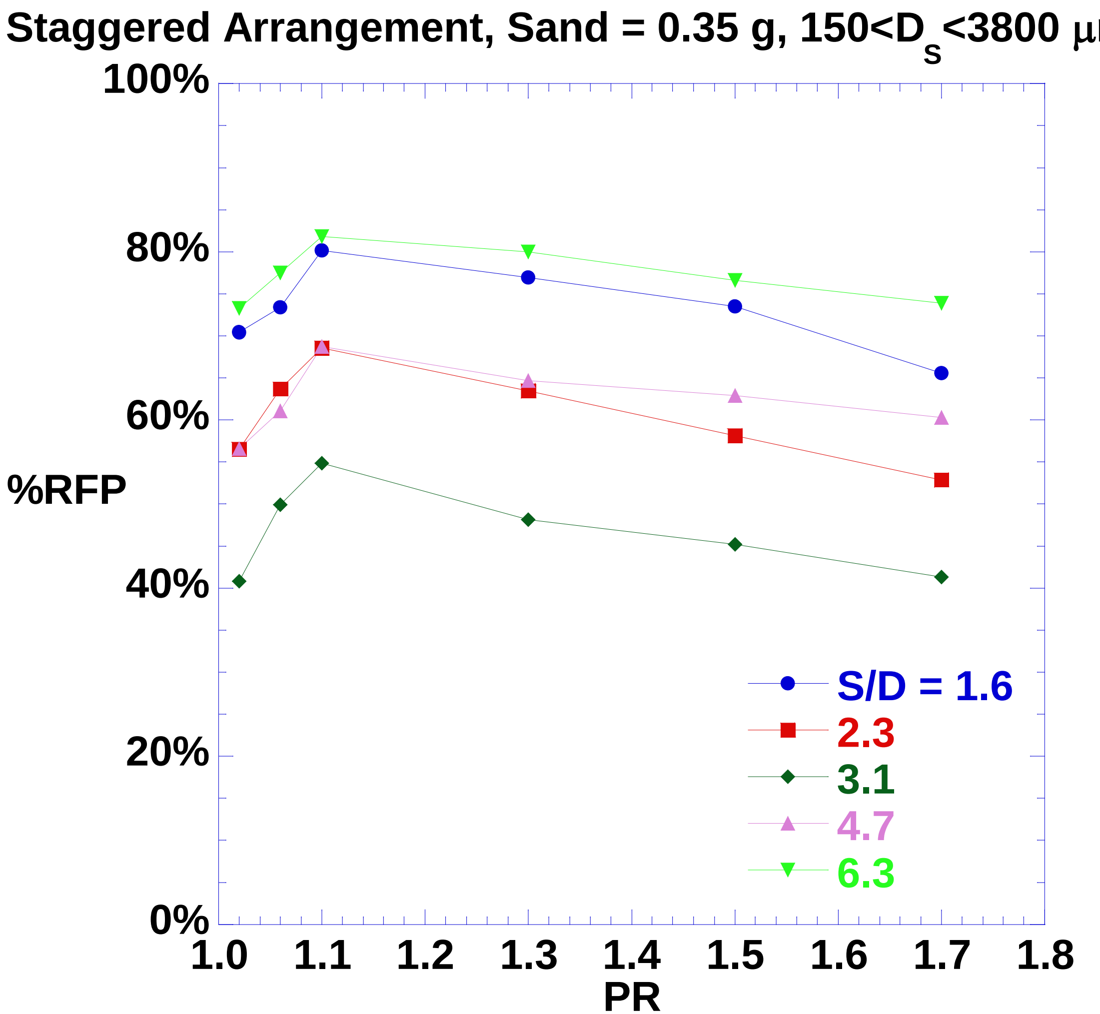

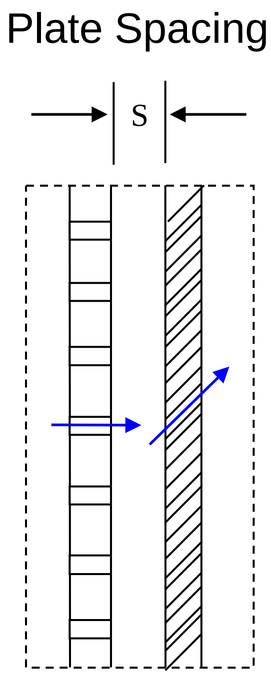

A similar trend for spacer thickness was seen with both staggered and aligned holes

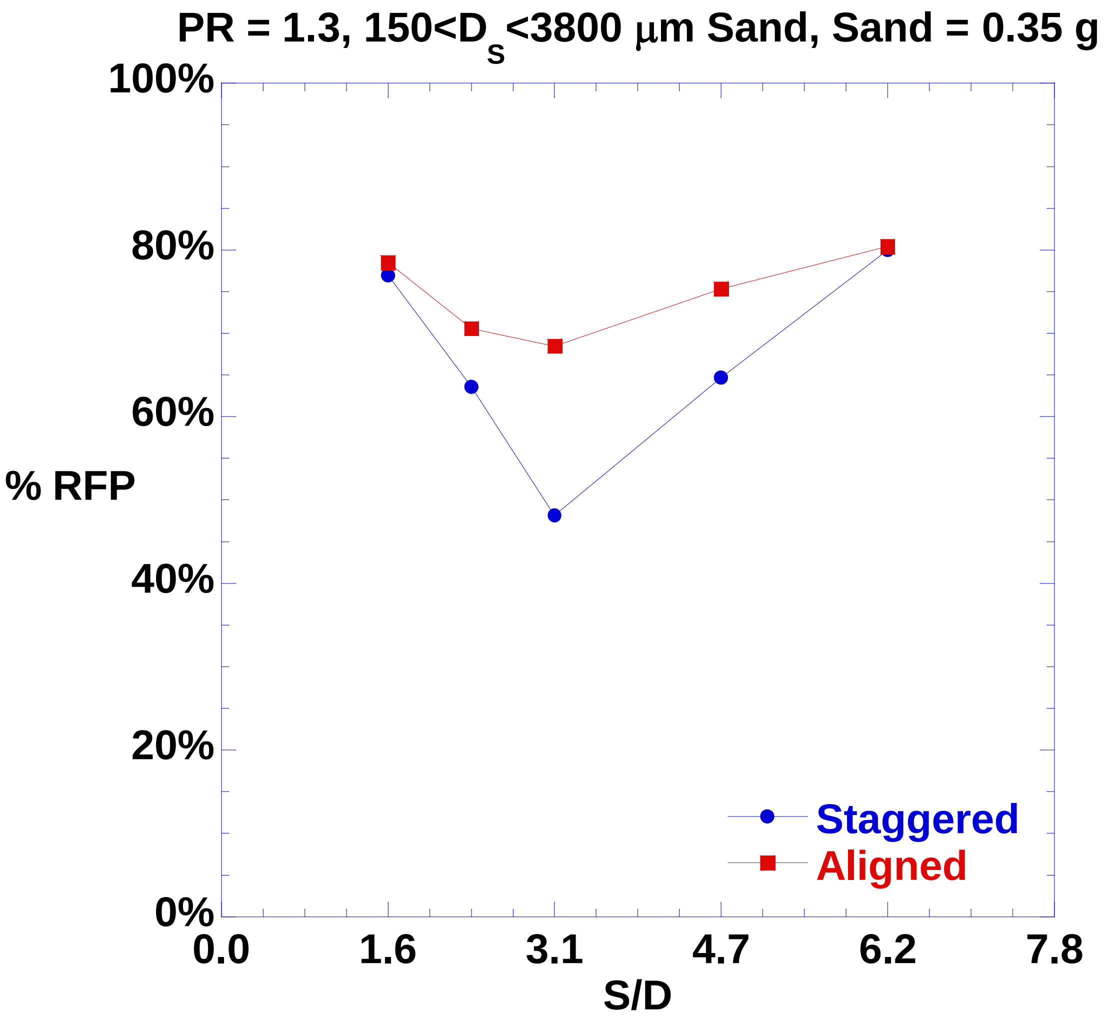

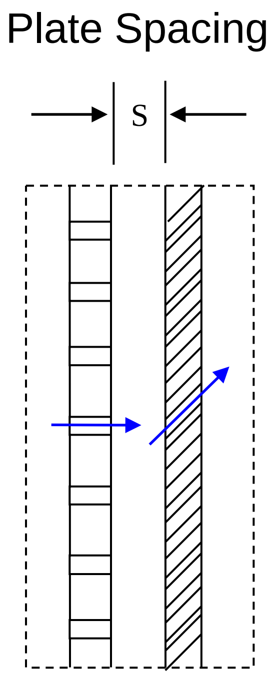

Rust can form in components along the flow path for secondary air used to cool the turbine blades

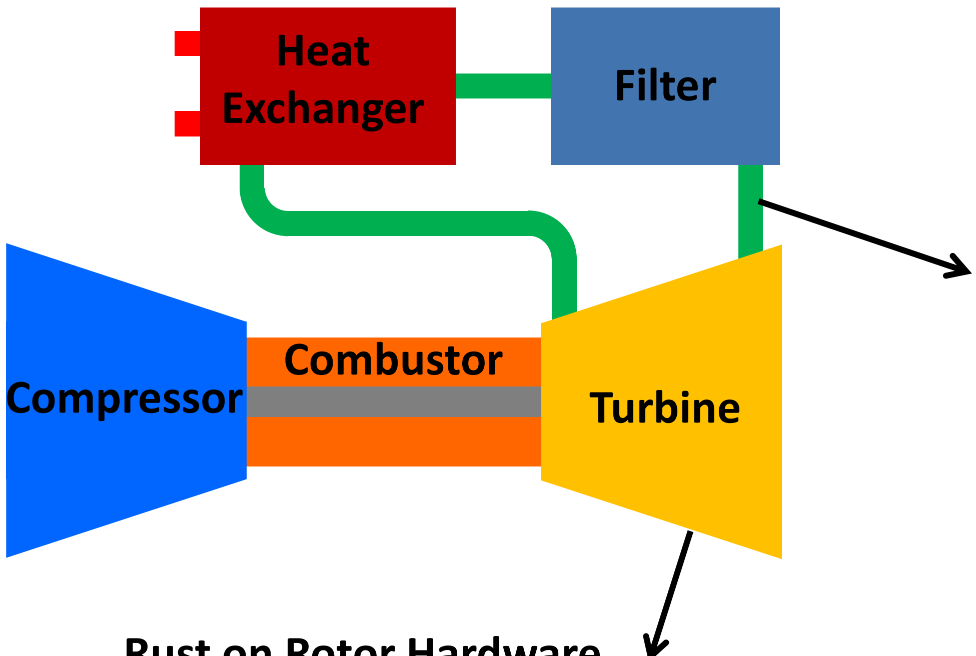

Rust in Secondary Air Piping

Rust on Rotor Hardware

http://powerccl.co.uk/turbine-corrosion.html

Rust particles entrained in the secondary flow can deposit in the axial seal pin region between blades

Secondary Flow at Axial Seal Pin

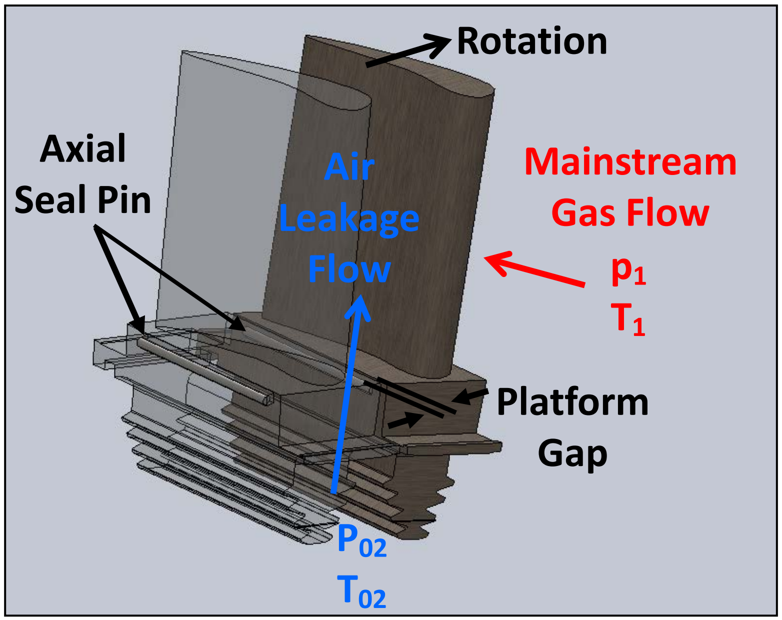

Purpose of seal pin is to:
- Prevent ingress of mainstream gas flow
- Damping mechanism

Particle deposition in seal pin leads to:
- Flow blockage and particle conglomeration
- Prevents free movement of pin

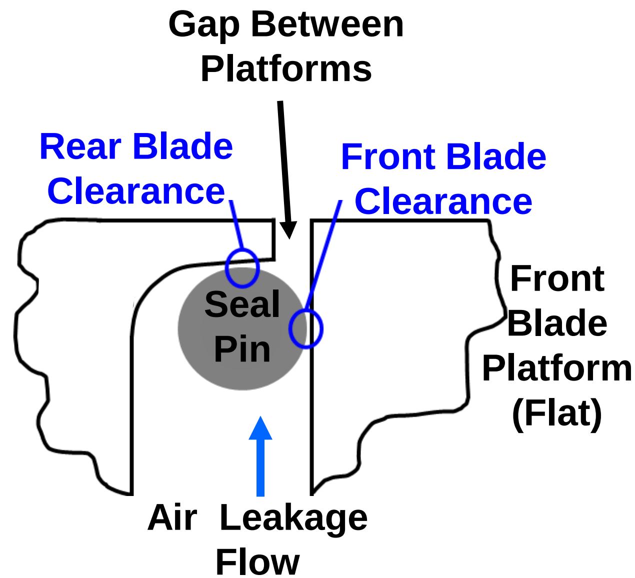

Effects of temperature and compaction due to rotation were evaluated for an axial seal pin

Effects of rust on static engine hardware

Effects of temperature and rotation on rust particles

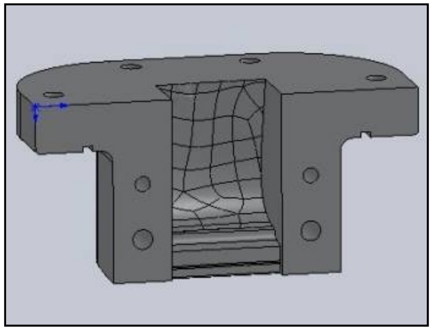

Development of a rotating facility and method

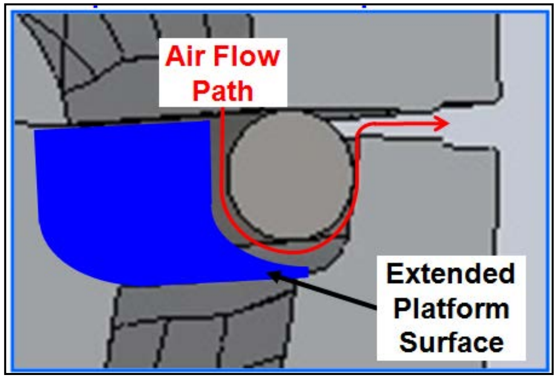

Effects of rotation on rust deposition

Flow blockage was found to increase with pressure ratio due to particle lodging at high velocities

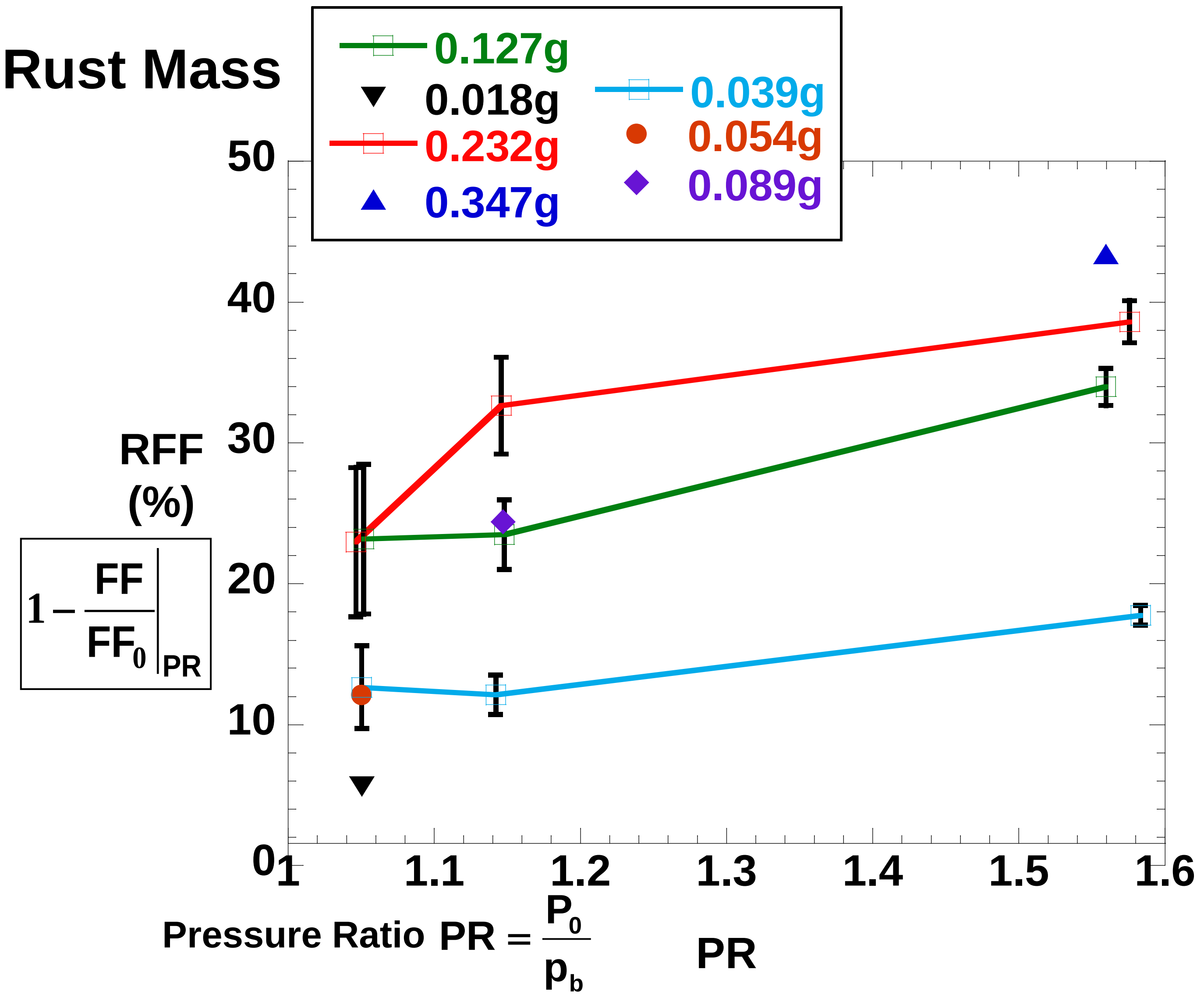

Some key physical observations resulted from tests of the metal oxide compounds at high temperatures

Most changes take place above 1500°F

Prolonged exposure to high-temperatures yielded similar results with shorter exposure

unheated

heated to 850°C (1560°F)

Particles conglomerate into large chunks at temperatures between 1700-2000°F (955-1093°C)

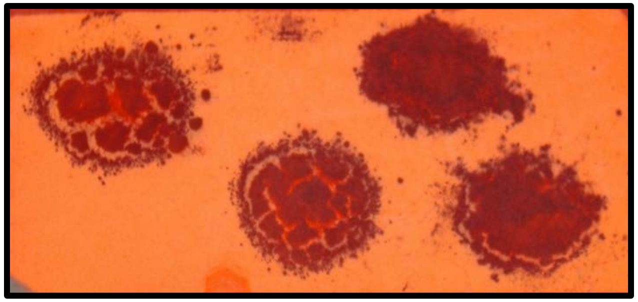

Red iron-oxide Fe_2O_3 turns black at elevated temperatures

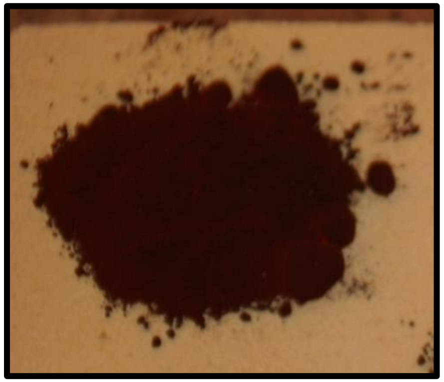

Turbine-representative rotational forces resulted in significant compaction of rust particles

$$\Omega = \frac{\text{centrifugal acceleration}}{\text{turbine centrifugal acceleration}}$$

	r (mm)	ω (rpm)	a_c (x g)	Ω
turbine first row	856	3,600	12,400	1
centrifuge	108	10,000	12,100	1

Before centrifuging: ρ = 0.9 g/cm^3

After centrifuging: ρ = 2 g/cm^3

Sample tube

Rust particles

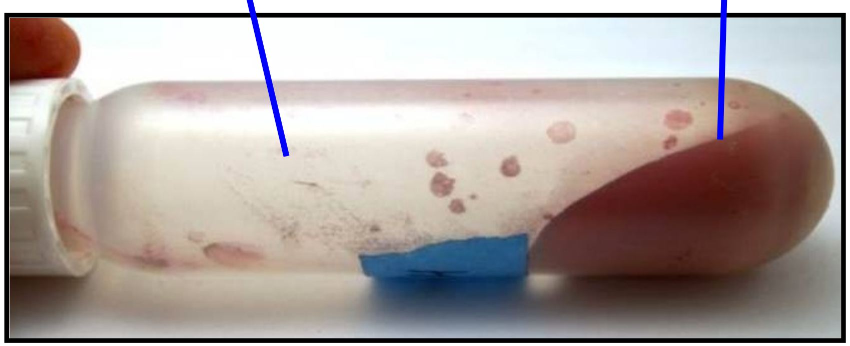

The effects of the centrifuge were similar on previously heated and unheated samples and for rotating speeds corresponding to Ω = 1 and Ω = 6

A modified centrifuge simulated effects of rotation; surface roughness was matched on specimens

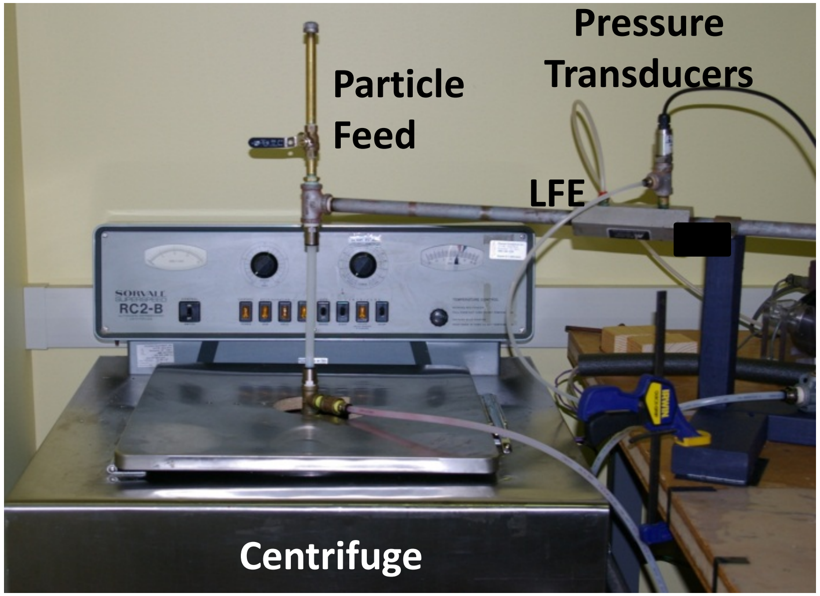

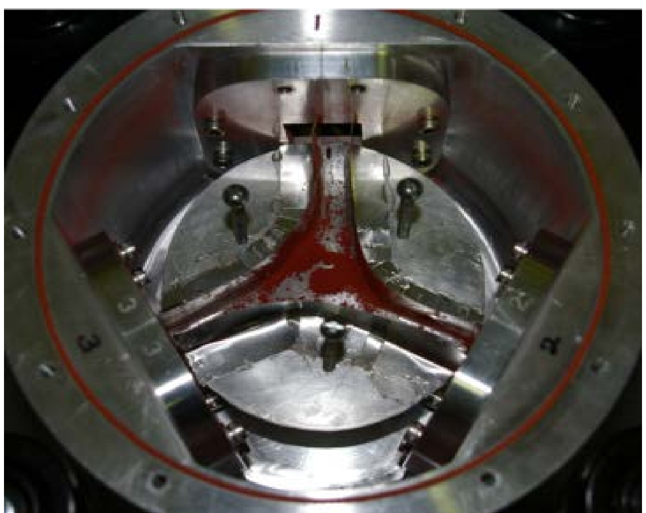

Particle Diffuser Plate

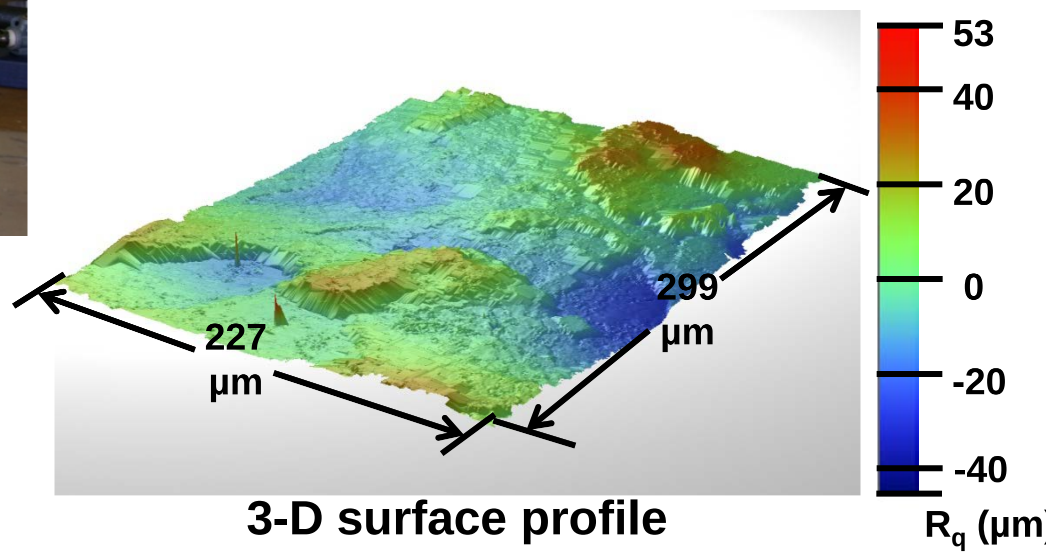

3-D surface profile

The flow function was similar for each of the three test coupons and scaled with the flow area

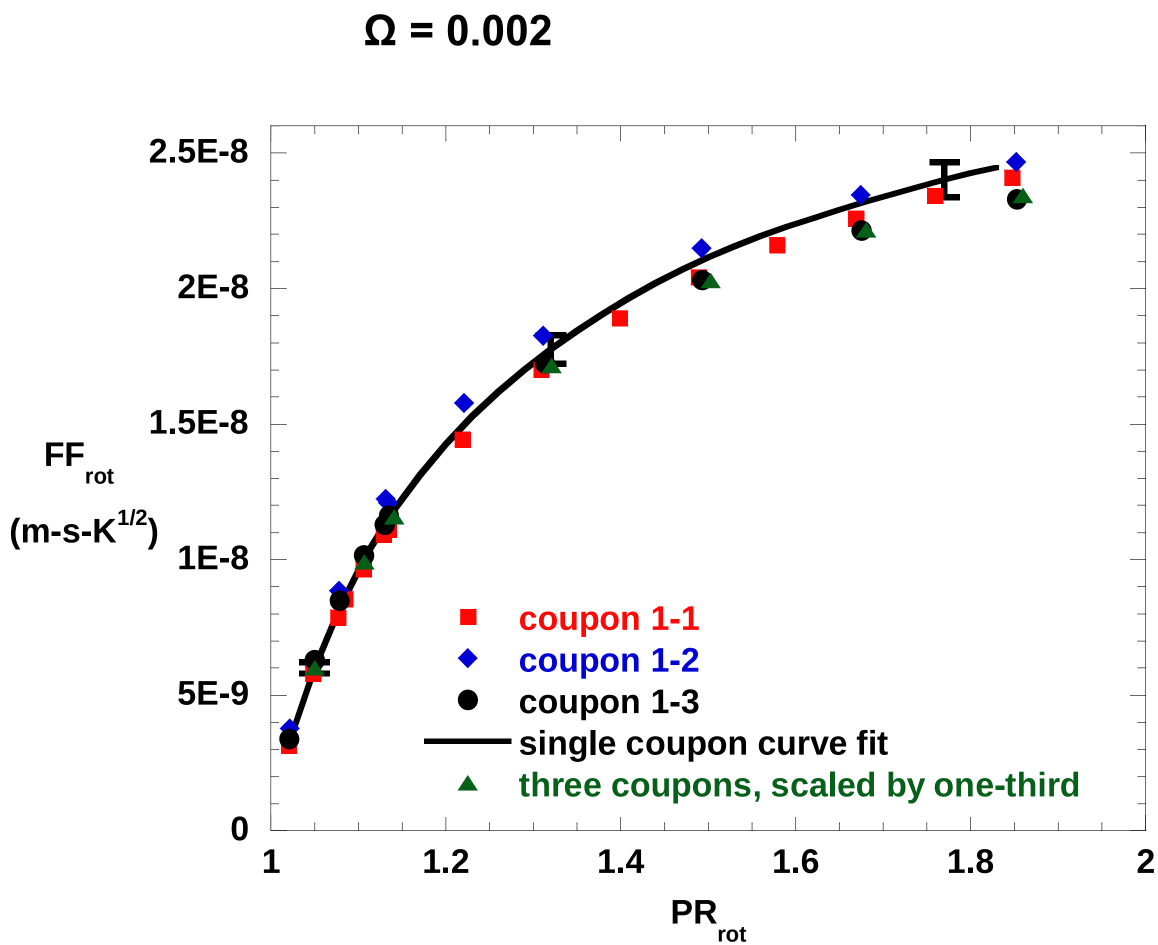

Test Configurations
(Top View of Chamber)

After injection, particles sizes were analyzed showing deposits near seal pin to be smaller

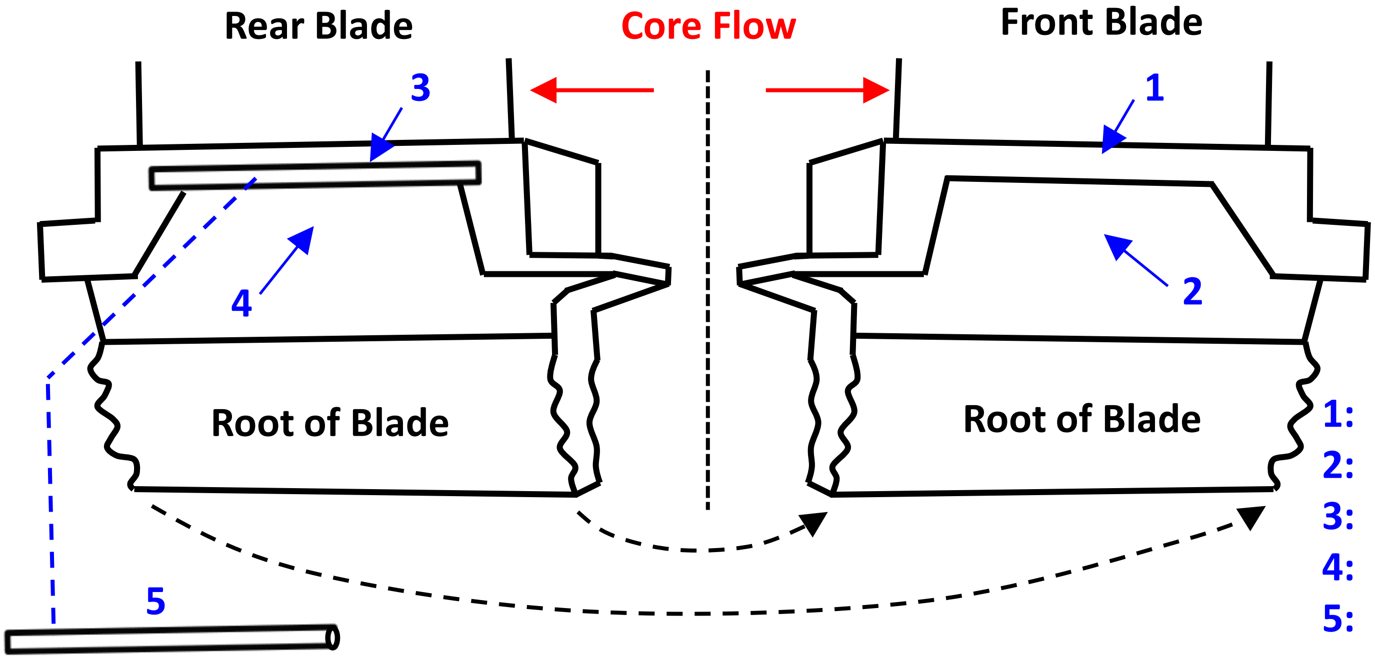

1: Pin– Front Blade
2: Contoured Area– Front Blade
3: Seal Pin Slot – Rear Blade
4: Contoured Area– Rear Blade
5: Seal Pin

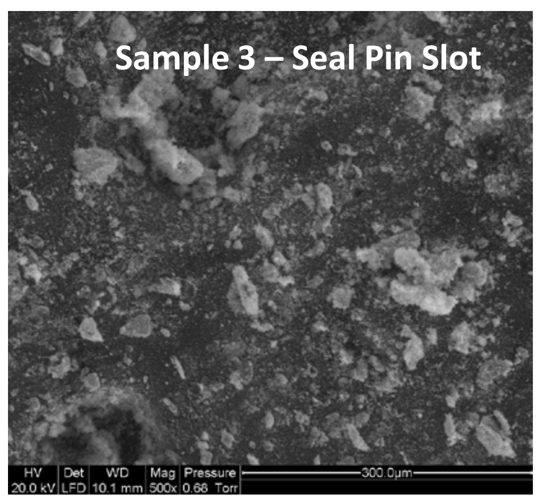

Flow blockages were nominally independent of rotational forces for this particular geometry

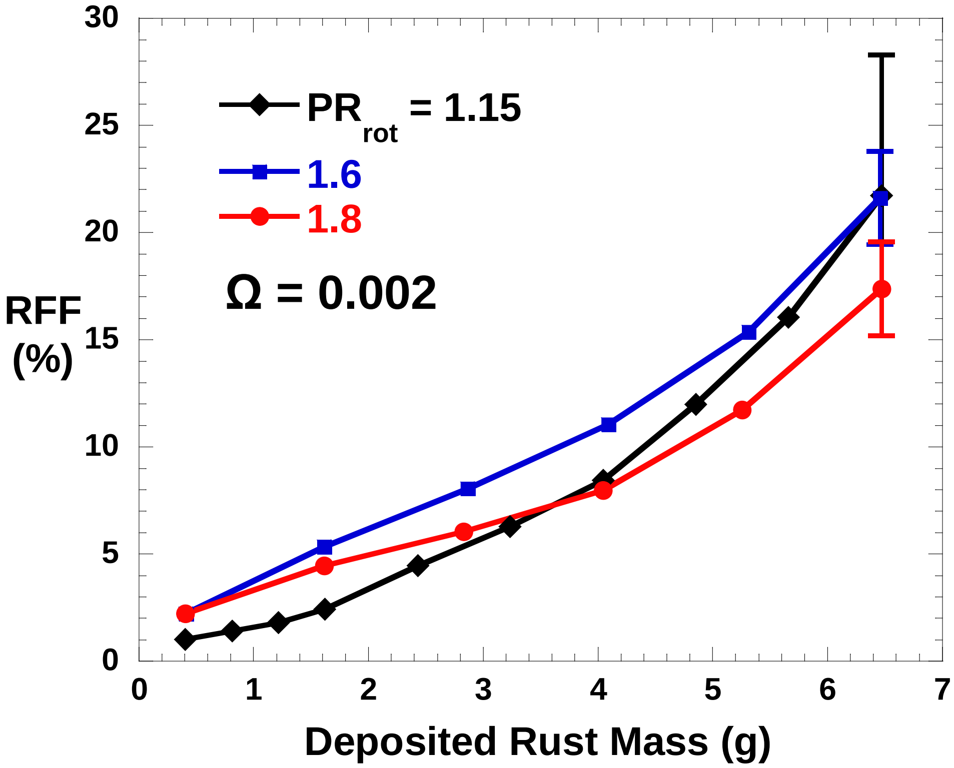

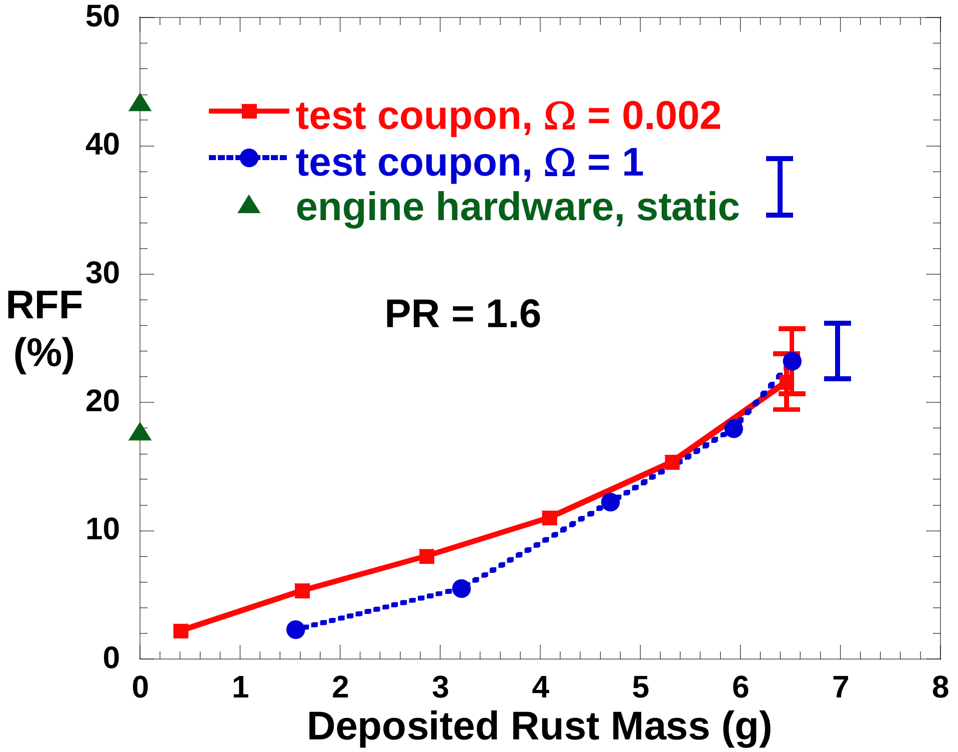

Each data point represents an average of at least three tests, each test with flow through three identical test coupons

RFF measurement uncertainty: ±9% of measured value

RFF repeatability for 3-test average: ±7% (95% confidence interval)

In conclusion, the effects of deposition can have profound impacts on heat transfer

Trenches and endwall contouring can help to mitigate the negative effects of deposition on cooling effectiveness

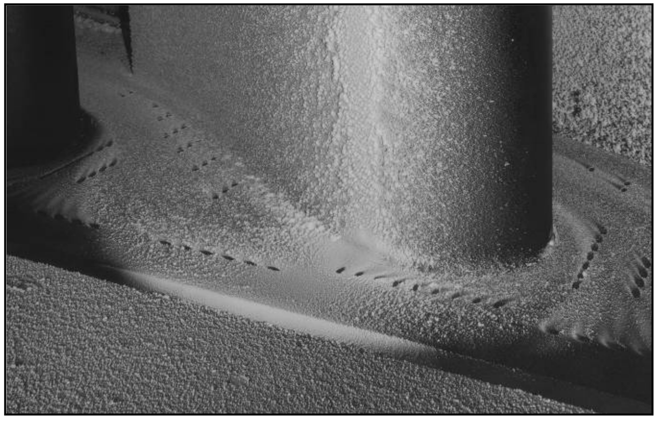

Double-walled liners can be designed to reduce blockages

Centrifugal effects can be important in some designs

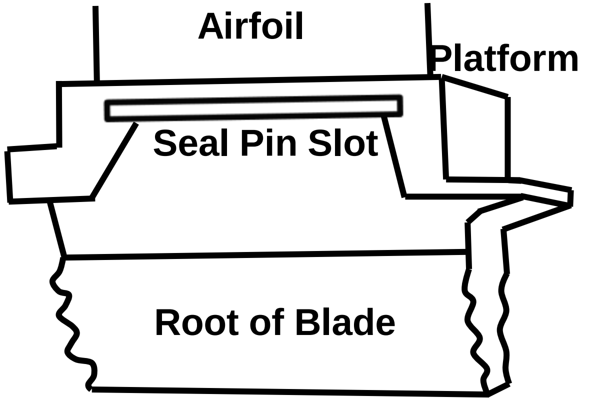

Testing is needed to determine what the effects might be!

Those who really do all the work…..

And…Seth Lawson, Nick Cardwell, Cam Land, Scott Walsh, Steve Lynch, Duane Breneman

In conclusion, the effects of deposition can have profound impacts on heat transfer

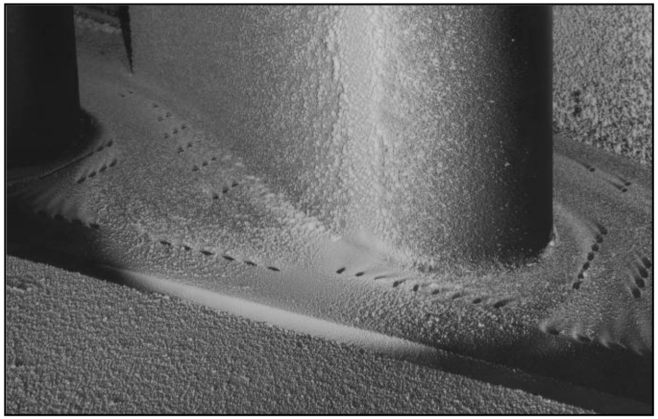

Trenches and endwall contouring can help to mitigate the negative effects of deposition on cooling effectiveness

Double-walled liners can be designed to reduce blockages

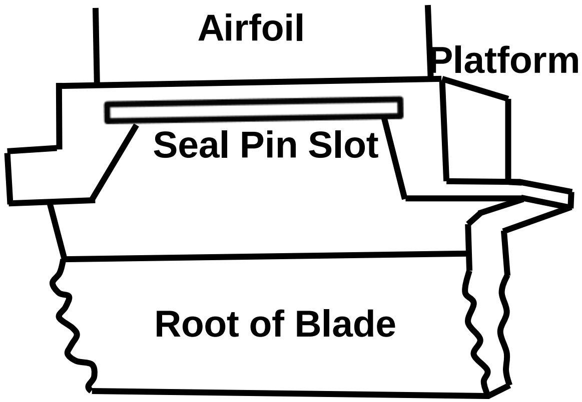

Centrifugal effects can be important in some designs

Testing is needed to determine what the effects might be!

Back-Up Slides

Wax droplets were tracked in the Lagrangian frame as discrete particles with simulated dispersion

$$\frac{du_{p,i}}{dt} = \frac{\sum F_i}{m_p}$$

$$= F_D\left(u_i - u_{p,i}\right) + \frac{g_i\left(\rho_p - \rho\right)}{\rho_p} + \frac{\rho}{\rho_p} u_{p,i} \frac{\partial u}{\partial x_i}$$

Particle Accel. = Drag force (Stokes' Law) + Gravity + Pressure gradient

$$F_D = \frac{18}{\rho_p d_p^2} \frac{C_D \mathrm{Re}_d}{24}$$

$$C_D = a_1 + \frac{a_2}{\mathrm{Re}_d} + \frac{a_3}{\mathrm{Re}_d^2}$$ [Morsi & Alexander, 1972]

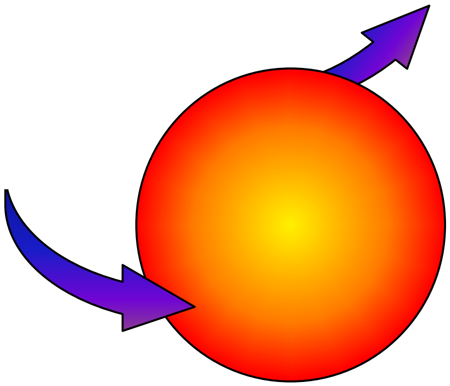

Heat transfer:

Lumped capacitance

$$m_p C_p \frac{dT_p}{dt} = hA_p\left(T - T_p\right)$$

Simulated turbulent dispersion:

Discrete Random Walk (DRW)

Random gas phase fluctuating velocity

$$u_i = \overline{u_i} + u_i'$$

$$u_i' \approx \mathrm{rand} * \sqrt{2k/3}$$

Solidification process model

$$\int hA_p\left(T_{p,s} - T\right)dt = m_p h_{fusion}$$

Flow visualization was performed with a high speed camera and Nd:YLF pulsed laser

Laser Frequency ~ 6kHz
Camera Speed = 2 kHz

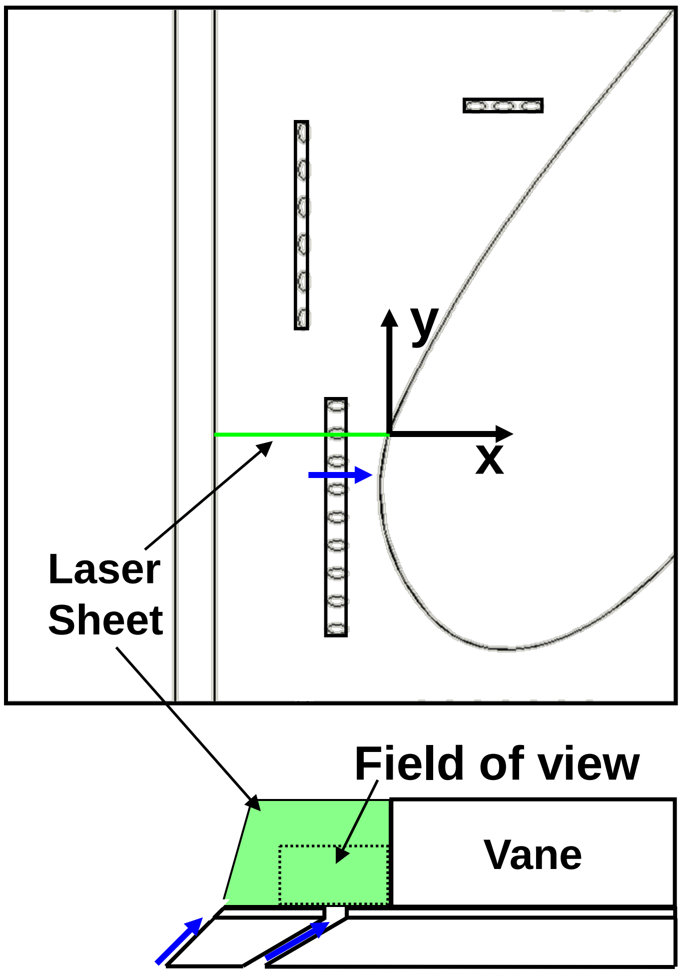

Composite images ~ 20 Frames (0.01s)

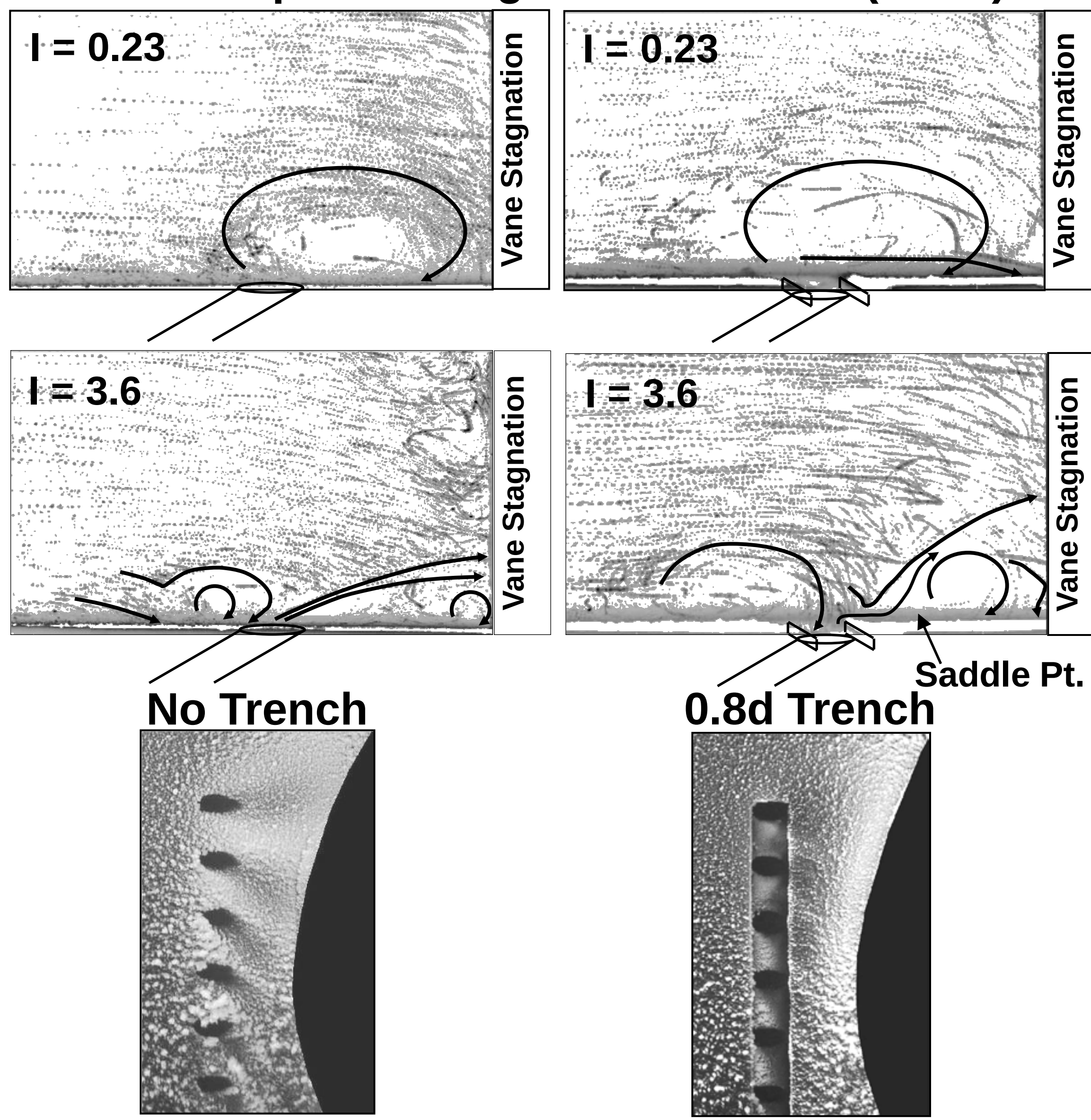

EAR Export Classification: ECCN 9E991

Digital pictures showed effects upstream of the film-cooling plate of the varying spacer thicknesses

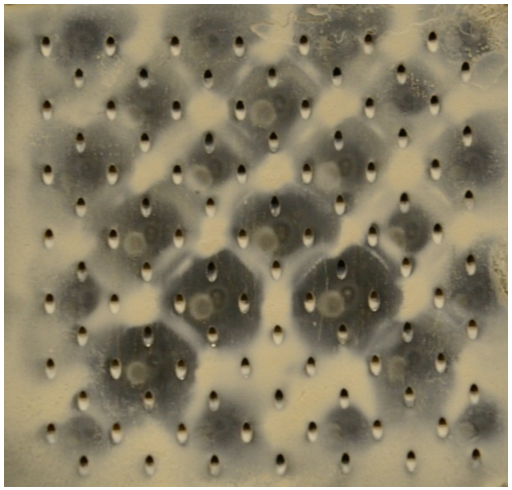

S/D = 1.6

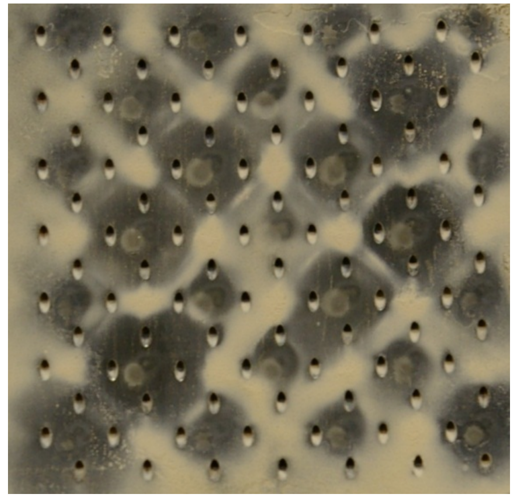

S/D = 2.3

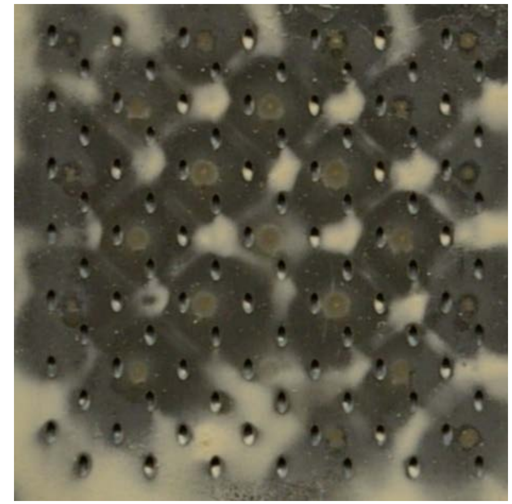

S/D = 3.1

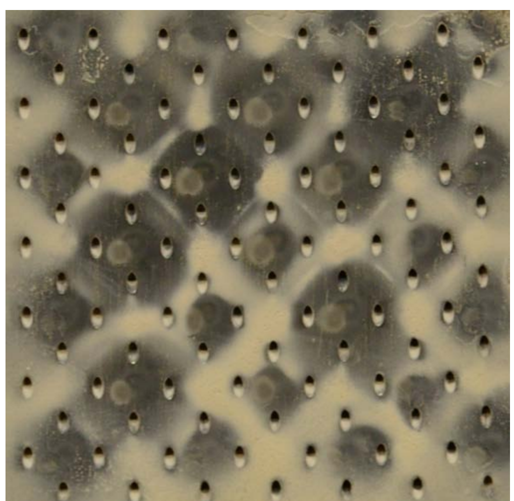

S/D = 4.7

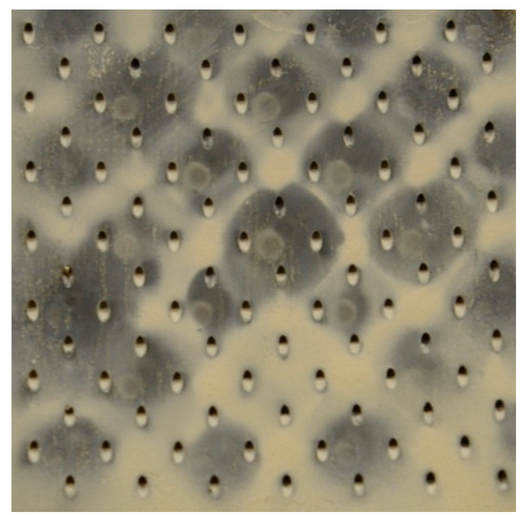

S/D = 6.3

Deposition varied with blowing ratio and was thickest near stagnation at M = 1.0

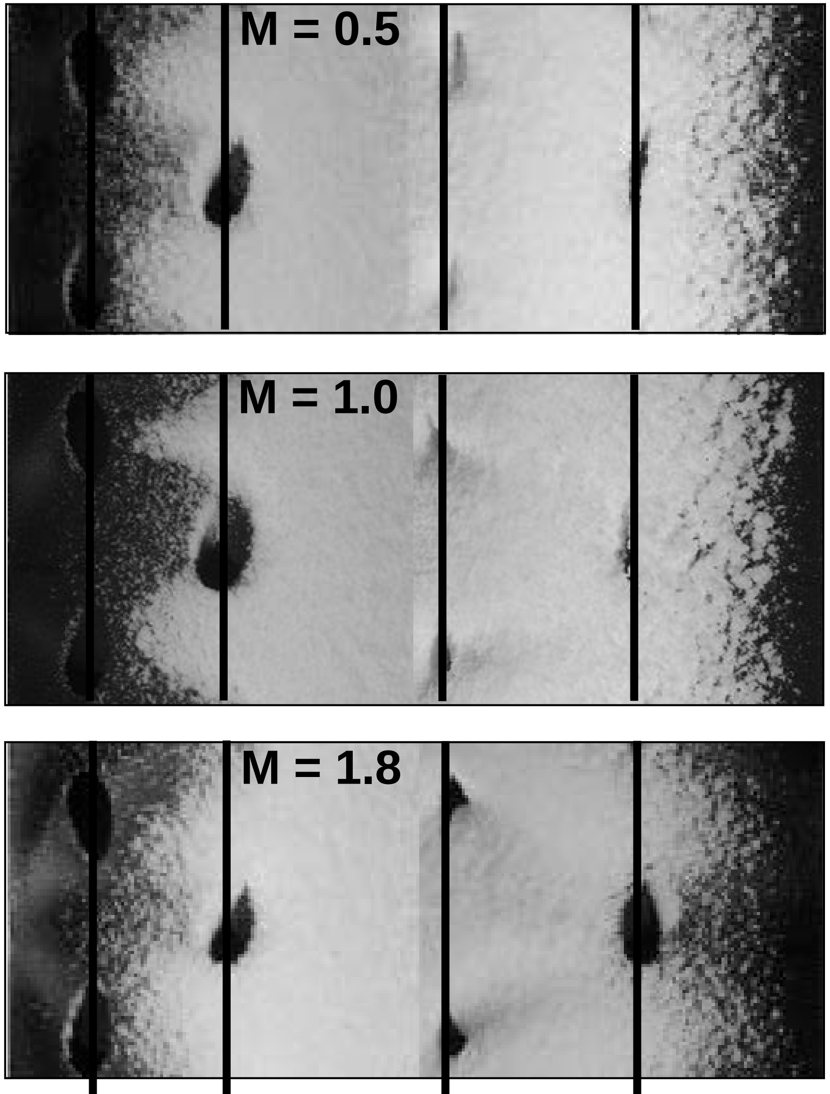

s/d = -6.0 s/d = -3.5 s/d = 1.2 s/d = 4.4

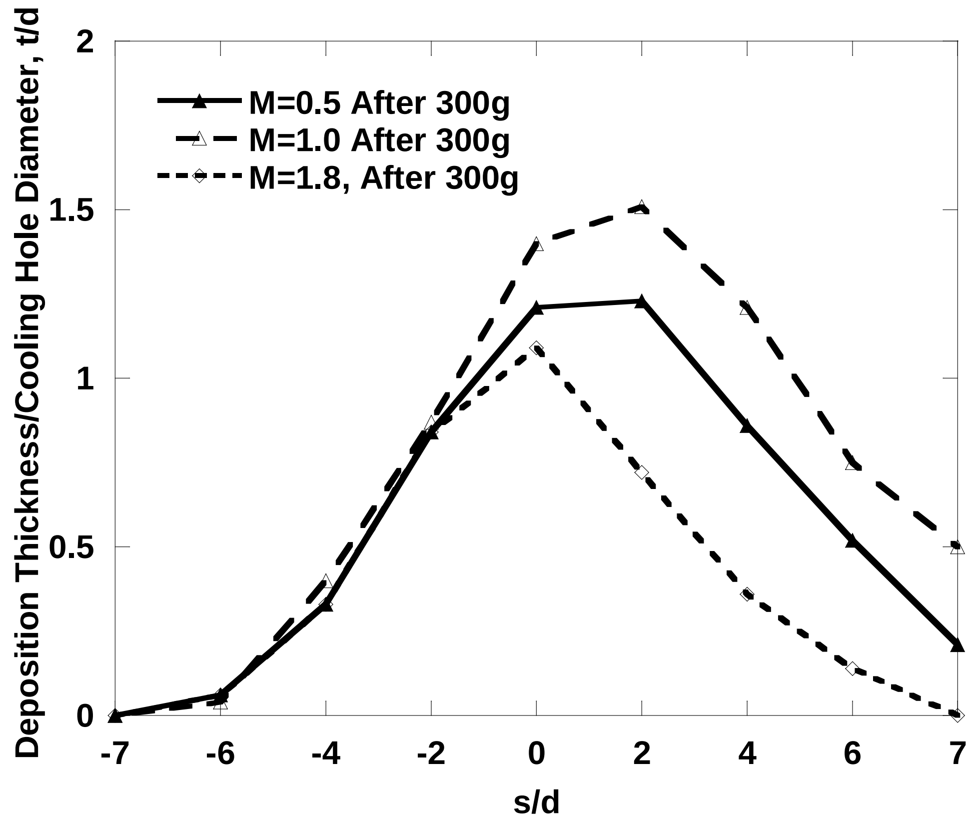

	M_L		
Cooling Row, s/d	M = 0.5	M = 1.0	M = 1.8
-6	1.2	1.4	2.0
-3.5	0.6	1.0	1.8
1.2	-0.7	0.4	1.5
4.4	0.9	1.2	1.9

Wax droplets were tracked in the Lagrangian frame as discrete particles with simulated dispersion

Discrete Phase Model - DPM
Volume Fraction = 7×10^{-7}
One-way coupling
Turbulent Dispersion – DRW

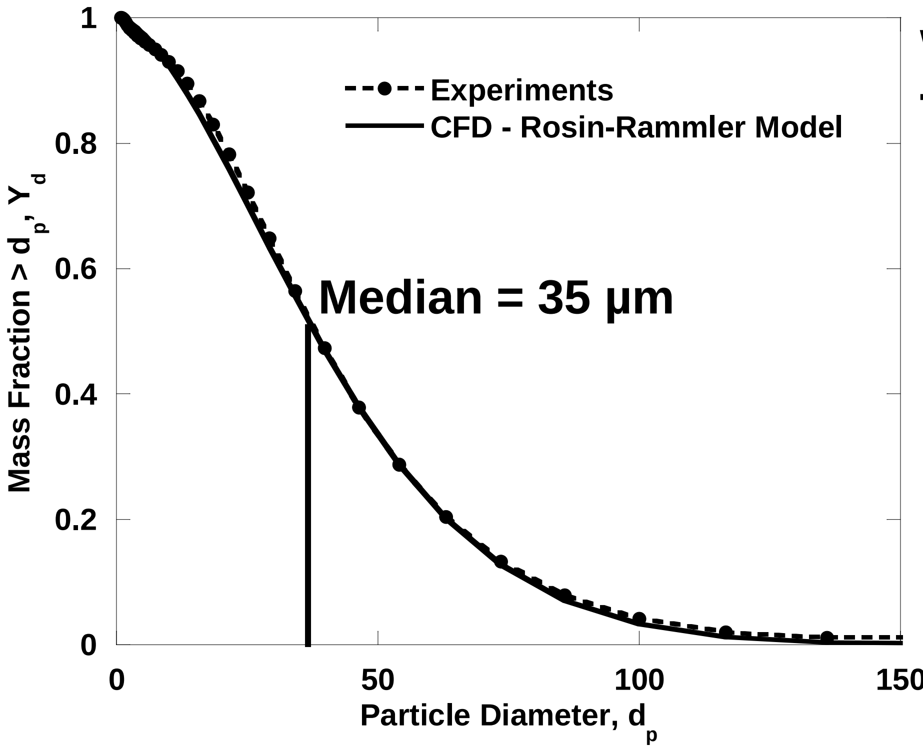

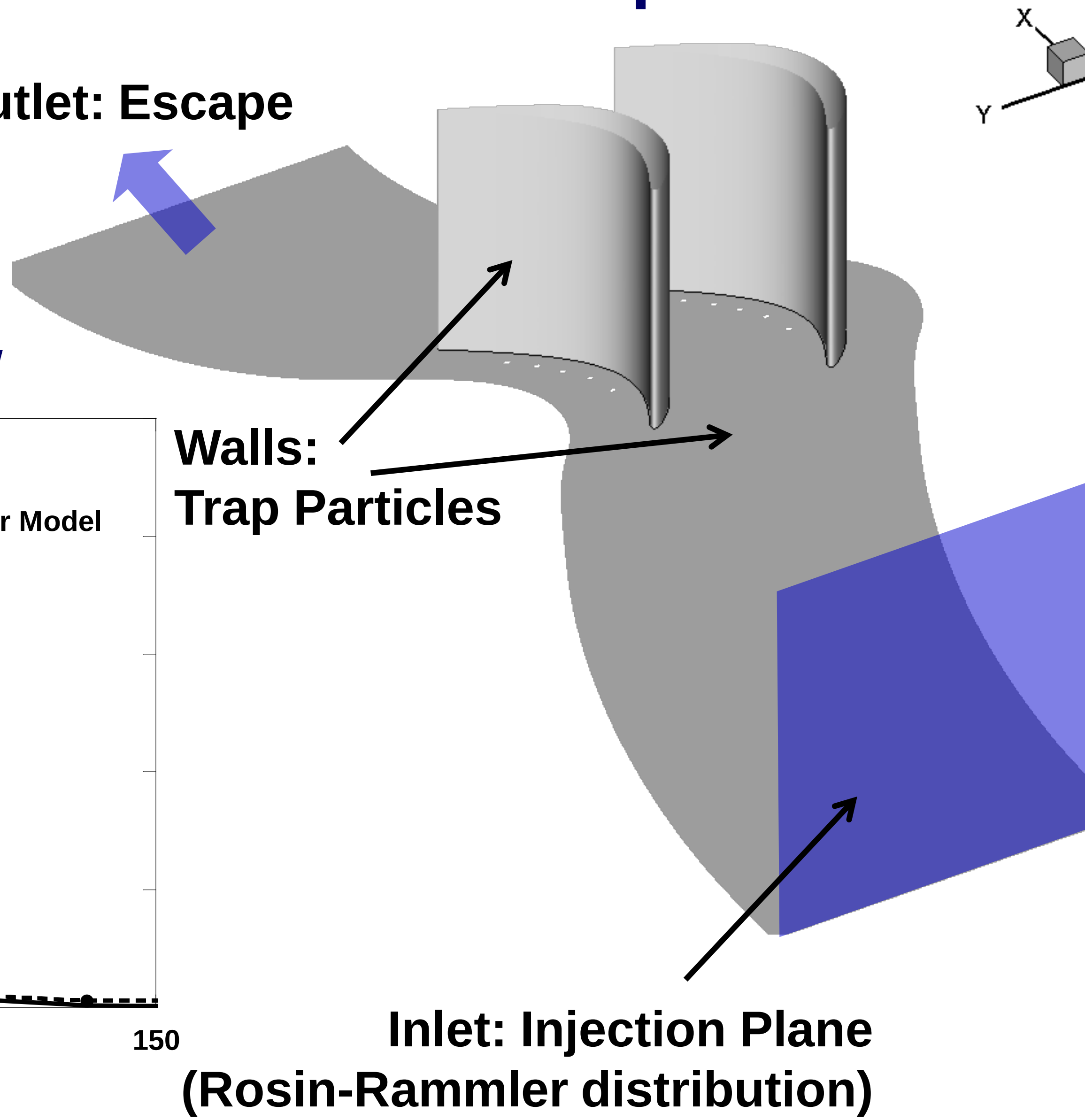

The sand diameter and densities dictate how the sand travels through the flow

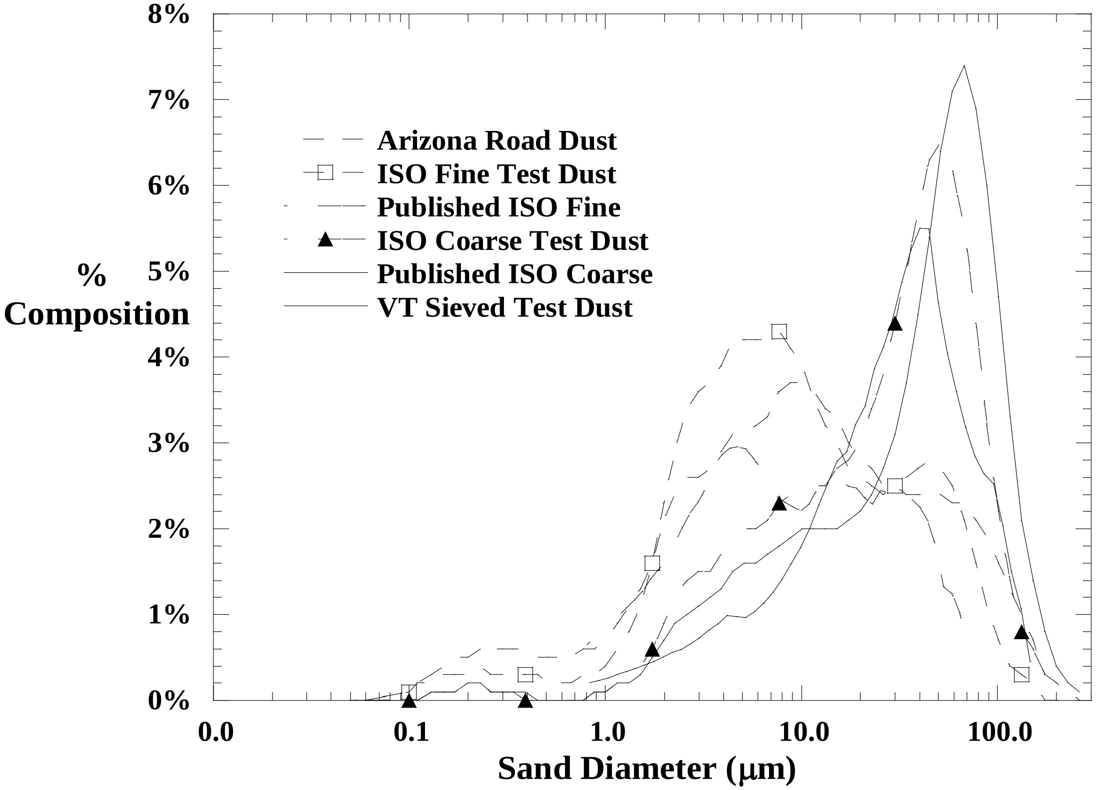

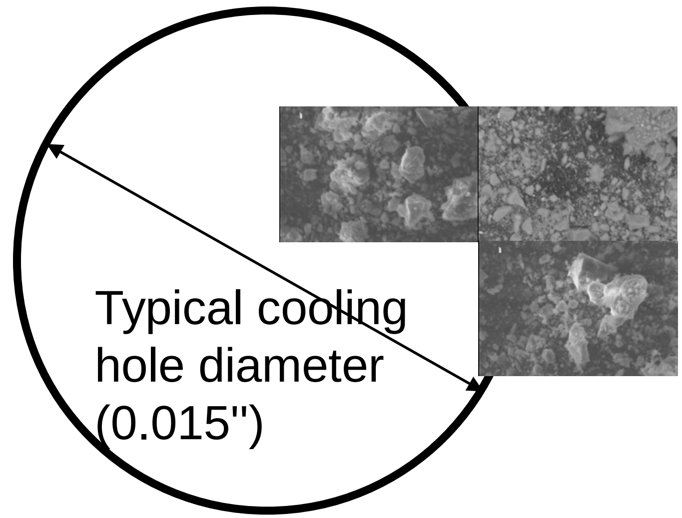

Sample	Density (g/cm^3)	Mean Diameter (μm)
Test Dust ISO 12103-1, A2 Fine	2.71	18.5
Test Dust ISO 12103-1, A4 Coarse	2.68	37.3
Sieved Test Dust	2.68	50.0

Sand ingested can deposit on internal surfaces blocking channels and roughening surfaces

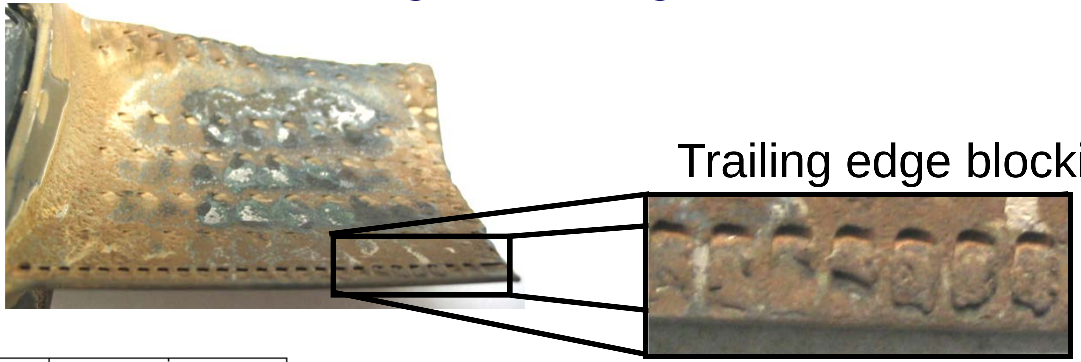

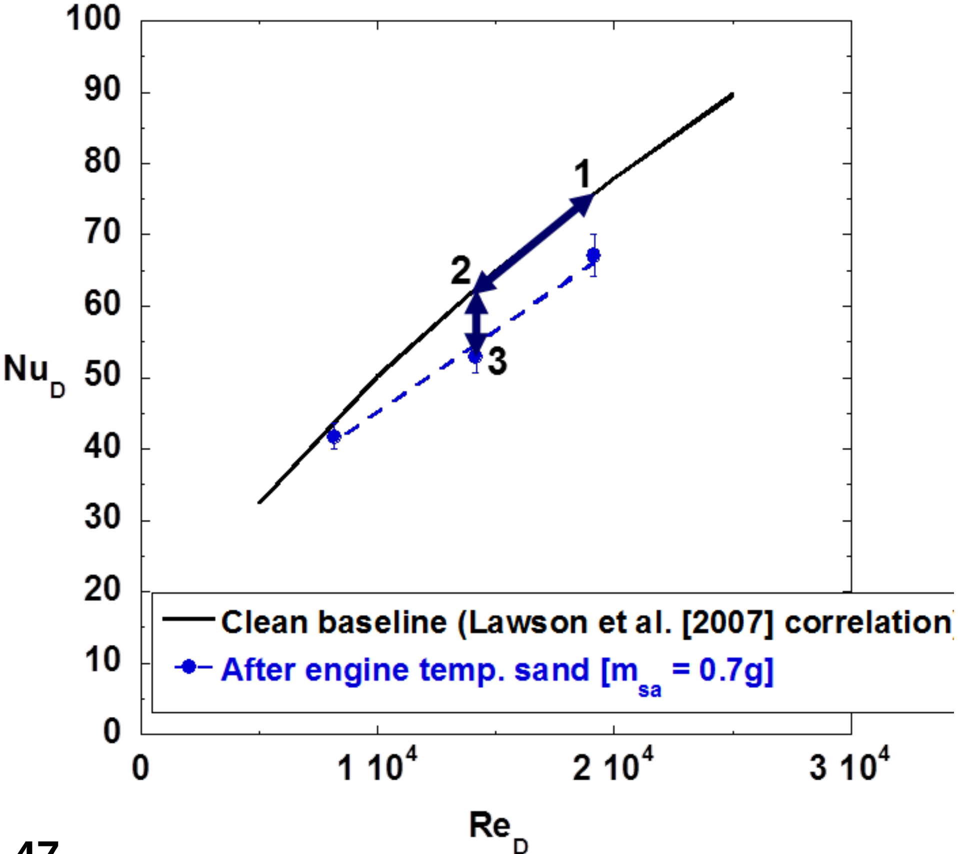

1→2 **(Re number decrease)**
For a given PR, the amount of air through a channel drops due to sand blockage

2→3 **(Nu number decrease)**
At the actual Re number, the Nusselt number also drops due to sand blockage

Overall heat transfer effect is between 5-10%

Leading edge cooling effectiveness increased with blowing ratio while coolant jets were attached

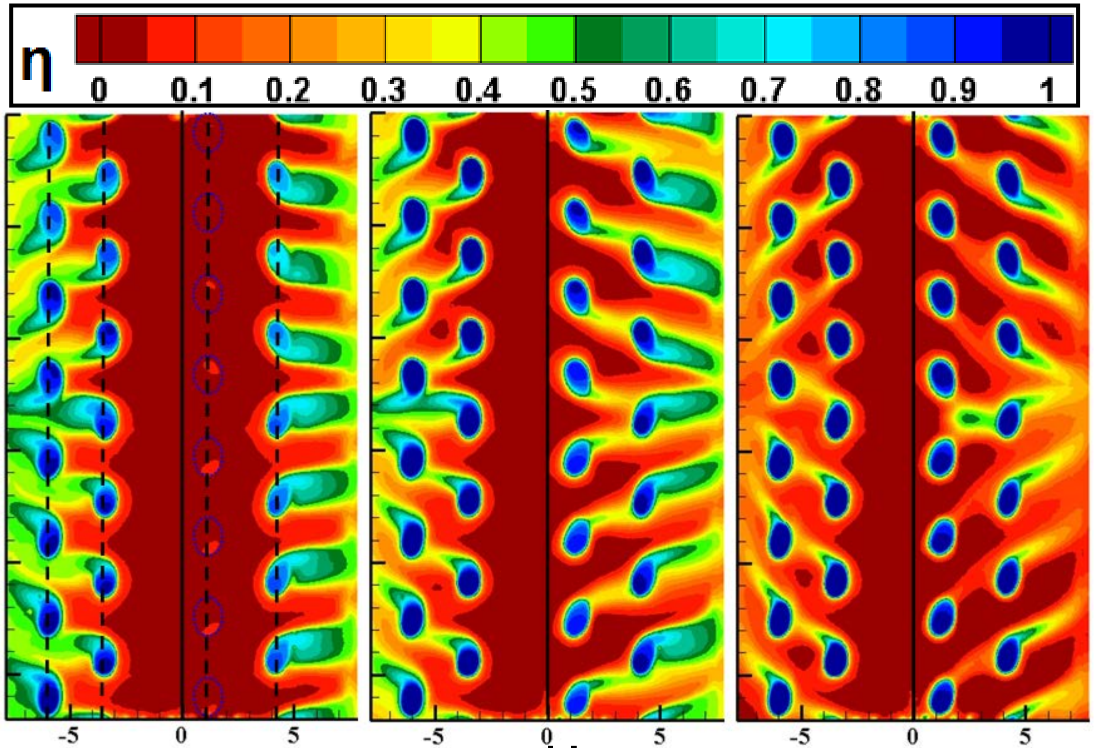

M = 0.5 M = 1.0 M = 1.8

No Deposition

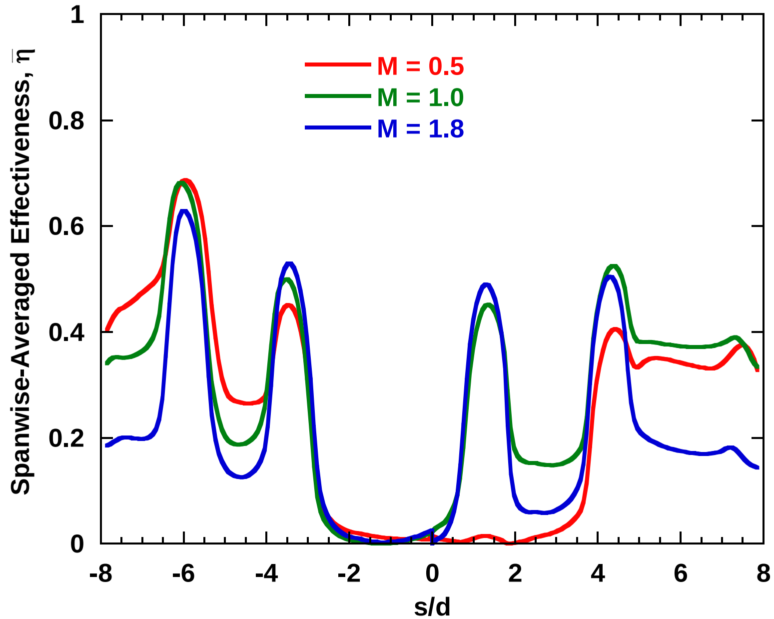

	M_L		
Cooling Row, s/d	M = 0.5	M = 1.0	M = 1.8
-6	1.2	1.4	2.0
-3.5	0.6	1.0	1.8
1.2	-0.7	0.4	1.5
4.4	0.9	1.2	1.9

$$M_L = \rho_c C_D \sqrt{2\left(p_c - p_{\infty,l}\right)/\rho_c} \Big/ \rho_\infty U_\infty$$

$C_D = 0.6$ [Byerly, 1989]

Deposition patterns were sensitive to trench depth having a strong correlation with coolant patterns

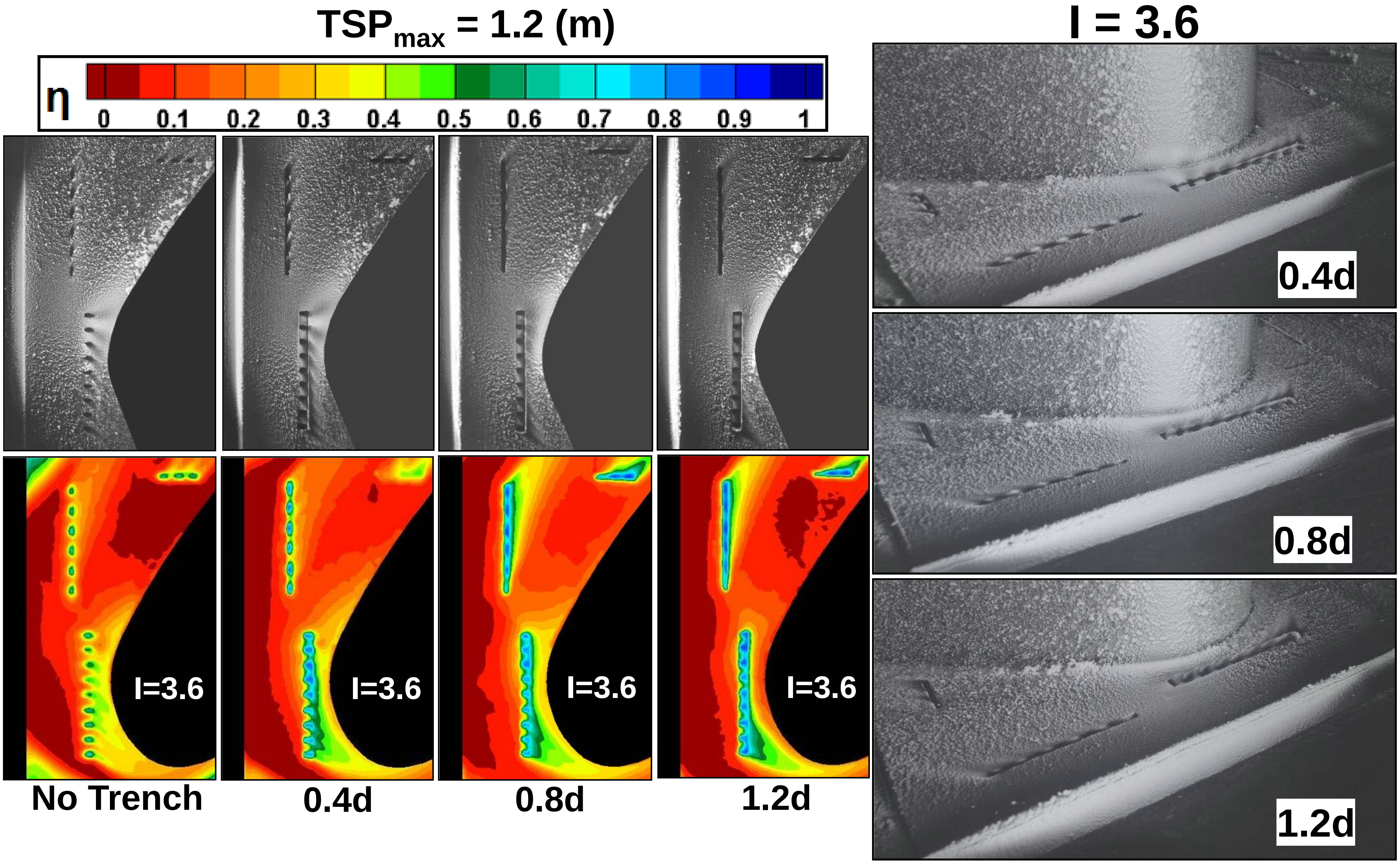

Impingement holes aligned with film-cooling holes caused increased blockage

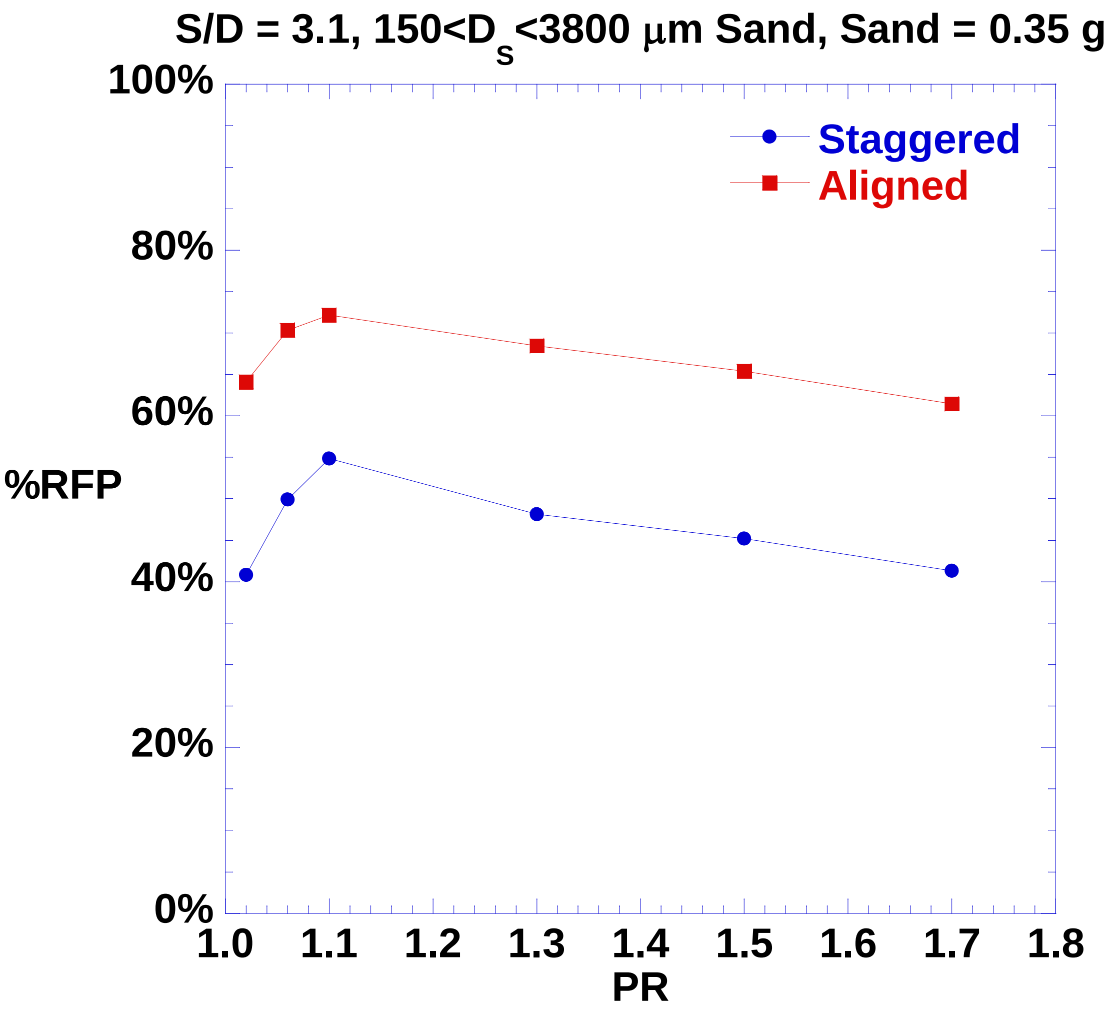

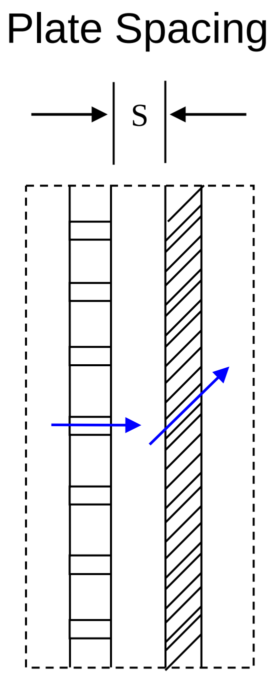

On an endwall effectiveness reduction was as high as 30% for passage cooling holes

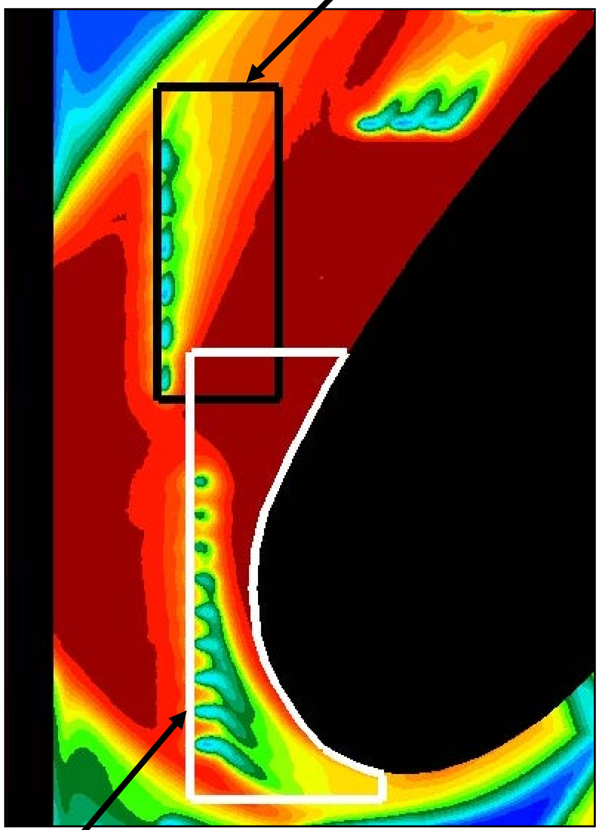

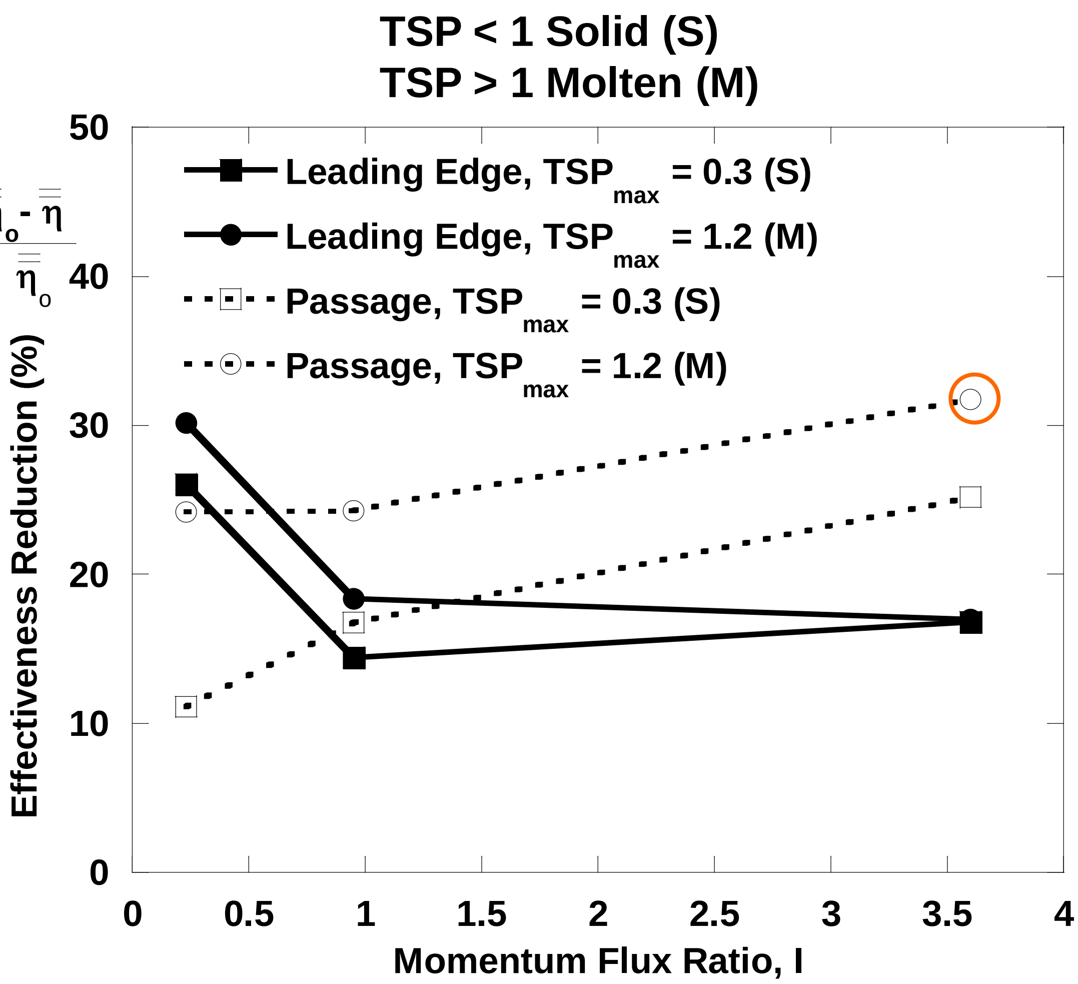

To simulate engine Stokes numbers, wax particles need to be 13x larger than fly ash particles

	Engine (Fly Ash)	Laboratory (Spa Wax)
Particle Density, ρ_p (kg/m^3)	1980	900
Inlet Gas Velocity, $U_\infty = U_p$ (m/s)	501	8
Gas Viscosity, μ (kg/m-s)	5.549×10^{-5}	1.852×10^{-5}
Hole Diameter, $d=L_c$ (cm)	0.17	0.635

Bons et al. [2001], Albert [2008]

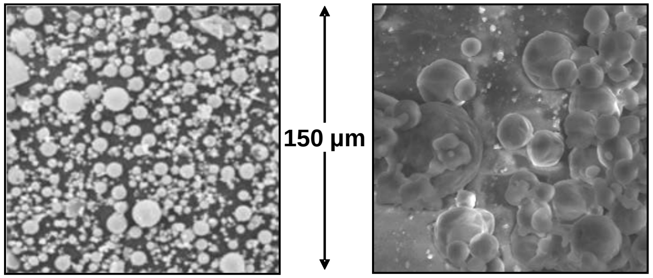

Fly Ash
Bons et al. [2007]

Spa Wax

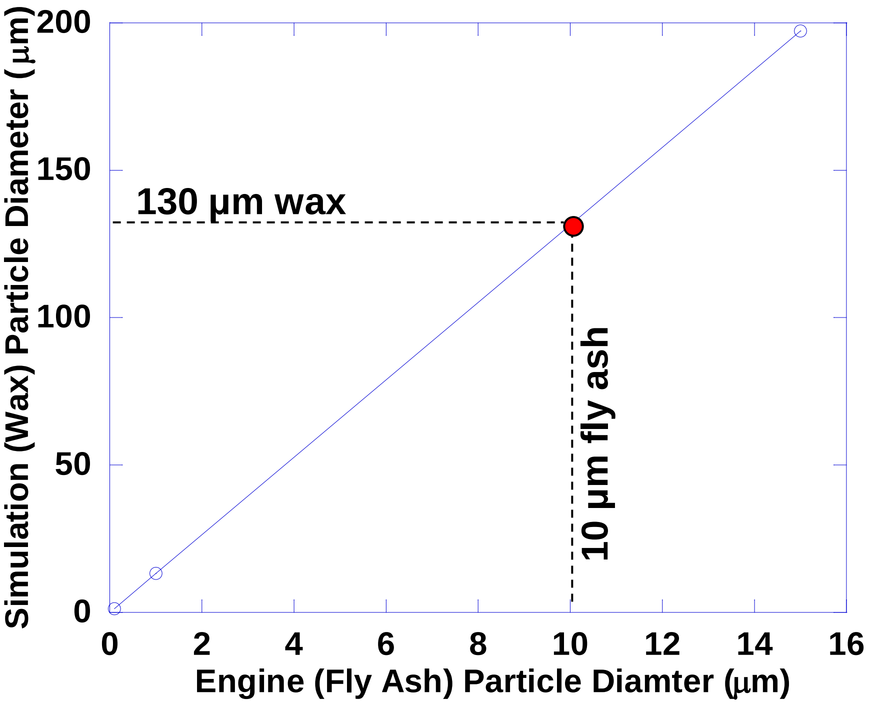

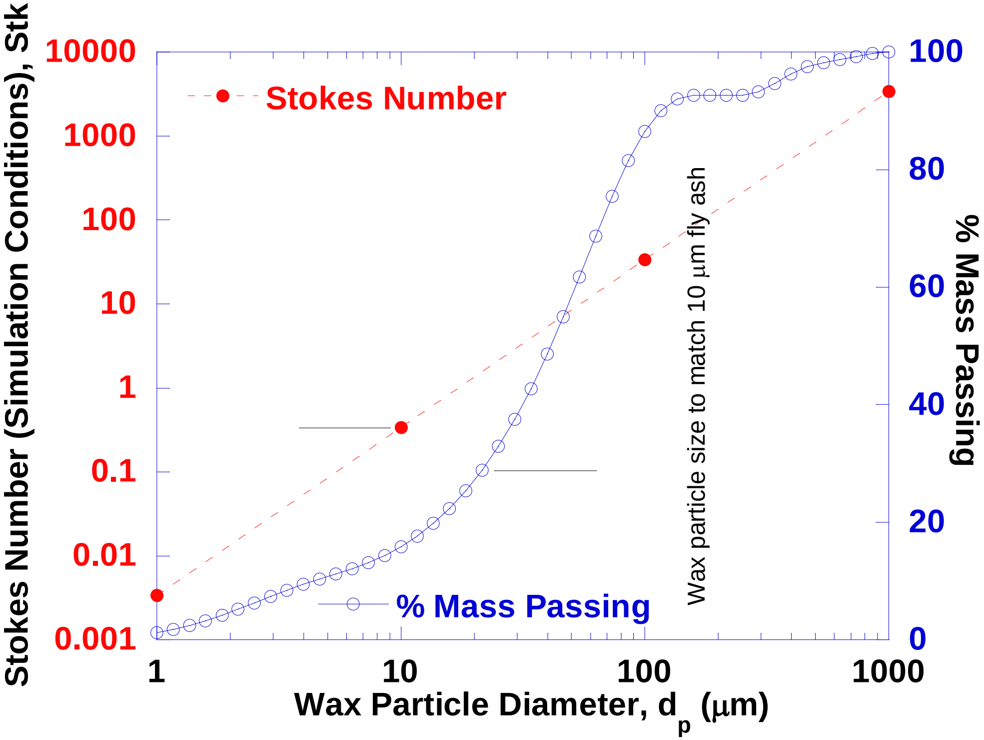

The methods used to dynamically simulate effects of deposition were applied in a wind tunnel facility

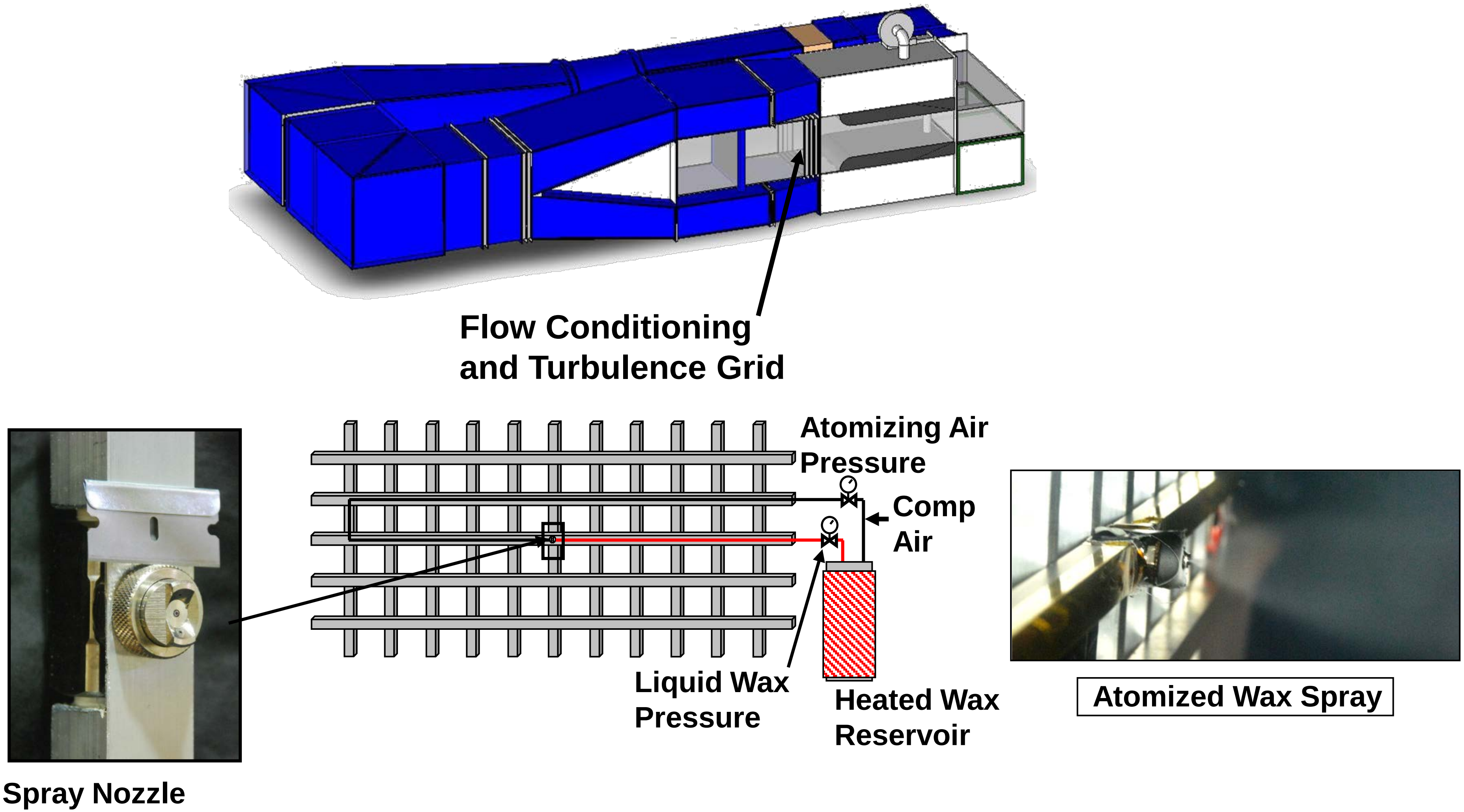

Typical experiments made use of gravity fed sand into the test coupons